NASA CONTRACTOR REPORT

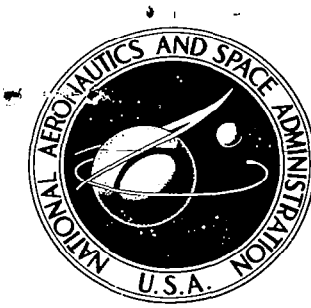

NASA CR-2349

ANALYSIS AND CALCULATION OF LIGHTNING-INDUCED VOLTAGES IN AIRCRAFT ELECTRICAL CIRCUITS

by J. A. Plumer

Prepared by
GENERAL ELECTRIC COMPANY
Pittsfield, Mass. 01201
for Lewis Research Center

NATIONAL AERONAUTICS AND SPACE ADMINISTRATION • WASHINGTON, D. C. • JANUARY 1974

1. Report No.	2. Government Accession No.	3. Recipient's Catalog No.
NASA CR-2349		

4. Title and Subtitle	5. Report Date
ANALYSIS AND CALCULATION OF LIGHTNING-INDUCED VOLTAGES IN AIRCRAFT ELECTRICAL CIRCUITS	January 1974
	6. Performing Organization Code

7. Author(s)	8. Performing Organization Report No.
J. A. Plumer	SRD 72-066
	10. Work Unit No.

9. Performing Organization Name and Address	11. Contract or Grant No.
General Electric Company 100 Woodlawn Avenue Pittsfield, Massachusetts 01201	NAS 3-14836
	13. Type of Report and Period Covered
12. Sponsoring Agency Name and Address	Contractor Report
National Aeronautics and Space Administration Washington, D.C. 20546	14. Sponsoring Agency Code

15. Supplementary Notes

Final Report. Project Manager, Paul T. Hacker, Aerospace Safety Research and Data Institute, NASA Lewis Research Center, Cleveland, Ohio

16. Abstract

This report describes an analytical investigation of techniques to calculate the transfer functions relating lightning-induced voltages in aircraft electrical circuits to aircraft physical characteristics and lightning current parameters. The analytical work was carried out concurrently with an experimental program of measurements of lightning-induced voltages in the electrical circuits of an F89-J aircraft. A computer program, ETCAL, developed earlier to calculate resistive and inductive transfer functions is refined to account for skin effect, providing results more valid over a wider range of lightning waveshapes than formerly possible. A computer program, WING, is derived to calculate the resistive and inductive transfer functions between a basic aircraft wing and a circuit conductor inside it. Good agreement is obtained between transfer inductances calculated by WING and those reduced from measured data by ETCAL. This computer program shows promise of expansion to permit eventual calculation of potential lightning-induced voltages in electrical circuits of complete aircraft in the design stage.

17. Key Words (Suggested by Author(s))		18. Distribution Statement
Lightning	Electronic equipment	Unclassified - unlimited
Aircraft accidents	Aircraft	
Electrical faults	Induced voltages	
		Cat. 02

19. Security Classif. (of this report)	20. Security Classif. (of this page)	21. No. of Pages	22. Price*
Unclassified	Unclassified	64	$3.50

* For sale by the National Technical Information Service, Springfield, Virginia 22151

TABLE OF CONTENTS

LIST OF FIGURES

LIST OF FIGURES (Continued)

LIST OF TABLES

SUMMARY

From measured lightning-induced voltages in aircraft electrical circuits, it has been possible to derive resistive and inductive transfer functions relating these voltages to the lightning current parameters. This derivation has been accomplished with a computer program, ETCAL, which was developed for this purpose several years ago when this analysis was first attempted, under NASA Contract NAS3-12019, the results of which were published in NASA CR-1744 (ref. 1) in 1970. The transfer functions obtained by the analysis of reference 1 were observed to be dependent upon the lightning current waveform, indicating a deficiency in the analytical procedure, since the airframe is believed to be comprised of inactive, linear elements whose characteristics remain the same regardless of current amplitude or waveshape. Since lightning currents are rapidly changing and of short duration, the time required for diffusion of such currents through the aircraft skin (e.g., skin effect) is probably significant, although it was not factored mathematically into the original transfer function analysis. In the belief that skin effect is significant, the transfer function analysis was refined in a continuation of this work sponsored by NASA under Contract NAS3-14836. A suitable representation of the time constant of skin penetration was obtained from the literature and factored into ETCAL, with the result that transfer functions now derived are more consistent throughout the range of lightning stroke waveshapes at which comparison data derived from other measurements was available. ETCAL has been re-written and is published in this report. With it, measured induced voltage data can be utilized to determine the resistive and inductive transfer functions relating lightning currents to voltages induced in an aircraft electrical circuit of interest.

At the same time, work was initiated on a completely analytical technique to arrive at the same transfer functions. This is a mathematical representation of an aircraft wing and a hypothetical electrical circuit conductor inside. Some simplifying assumptions relating to wing geometry and lightning current flow are made in the first attempt. The magnetic flux linking the circuit and flux density at the conductor location are calculated as functions of an assumed lightning current filament in the wing skin. The contributions from a large number of such filaments

assumed to comprise the wing are summed to obtain the total magnetic flux density and flux linking the line-integral path of the conductor and its airframe return. From this, the transfer inductance, M, is easily derived. The resistive transfer function, R_s, is calculated as a function of geometry and material resistivity, so it is the d-c resistance and not the effective resistance calculated by ETCAL. Realizing this, however, and estimating the effective resistance from it, the resulting values of R_s and M compared well with corresponding values obtained via ETCAL from measured induced voltages on a circuit inside an F89-J aircraft wing.

The prospects for refining WING to account for physical peculiarities such as resistive bonds, access doors, non-uniform lightning current flow and others appear promising, as well as the possibility of modeling other sections of airframe in this manner and combining them to represent a complete aircraft. The resulting tool would be a powerful means for aircraft designers to evaluate prospective electrical circuit compatibility in the lightning environment and eliminate potential lightning effects problems before they become troublesome on production aircraft.

INTRODUCTION

This report describes an analysis of lightning-induced voltages in aircraft electrical circuits. The work reported herein builds upon former analytical work performed under NASA Contract NAS3-12019, "Measurements and Analysis of Lightning-Induced Voltages in Aircraft Electrical Circuits" (ref. 1). In the present work, progress has been made towards two broad objectives:

1. Determination of the transfer functions relating measured lightning-induced voltages to lightning current and airframe parameters.

2. Development of a modeling technique for calculating lightning-induced voltages in various aircraft electrical circuits.

The need for a greater understanding of the transfer functions of objective (1) is apparent because these functions can ultimately tell us more about the various factors influencing the susceptibility of particular aircraft electrical circuits to lightning. In the previous experimental program, (ref. 1) a computer program (ETCAL) was developed which enabled the reduction of the resistive and inductive transfer functions, R_s and M, respectively, from measured oscillographic induced voltage data. In some circuits upon which measurements were made, a general correlation between aircraft structural characteristics and these transfer functions was apparent, but for other circuits, the meaning of them was unclear. In addition, the values of R_s and M were often dependent upon current waveshape - a fact which caused some discomfort since, in theory, transfer functions should be dependent upon the aircraft circuit and airframe physical characteristics only. Accordingly, further analysis work was performed under this contract to learn more about these factors. If these parameters can be understood in terms of tangible wing structure and wing electrical circuit characteristics, aircraft designers may be better able to design aircraft circuits which minimize lightning-induced voltages. The work accomplished toward this objective is presented in Section I of this report.

All research conducted in the former program was for the purpose of measuring and understanding the possible lightning-induced voltages in an existing airframe. Of even greater importance is the problem of determining the possible levels of lightning-induced voltages in new aircraft during the design stage. If a reliable technique were available for this purpose, aircraft designers could evaluate the consequences of various alternate

structural and electrical system designs as far as lightning is concerned. If the results showed unacceptable induced voltage levels, protection could be designed into the system or a remedial design modification utilized. The second objective of this program, therefore, was to formulate a simple analytical model of a basic airframe component and evaluate its authenticity. If successful, such a model would show the methods needed for later development of a more extensive model for use in aircraft design evaluations.

The main text of this report is divided into two sections. Section I covers the transfer function analysis and development of the computer program, ETCAL, to derive the effective transfer functions from measured induced voltage data. Section II describes the basic theory and development of a computer program, WING, to calculate the transfer functions for various electrical circuits enclosed within an aircraft wing. An Appendix includes the detailed mathematical derivations of the magnetic flux formulas utilized by the computer program, WING.

SECTION I - TRANSFER FUNCTION ANALYSIS

TRANSFER FUNCTIONS

A mechanism by which lightning can affect aircraft electrical and avionics systems is by the generation of magnetically-induced and resistive voltage rises within aircraft electrical circuitry. These voltages may or may not be harmful to the circuits themselves, as well as the avionics equipment to which these circuits are connected. Even if the aircraft has an electrically continuous metallic skin, its non-cylindrical geometry will enable some magnetic flux to be present within the wing and fuselage, even if all of the lightning current were to flow through the skin only. This magnetic flux will link electrical circuits within these enclosures, causing induced voltages. Similarly, the finite resistivity of the metallic skin will permit resistive voltage rises within the skin (or structure) along the path of lightning current flow. If an aircraft electrical circuit happens to employ the structure as return path, then this resistive voltage enters this circuit, in series with the magnetically-induced voltage in the same circuit and any other (normal) steady-state voltages present. Capacitively coupled voltages may also be produced in these circuits; however the essentially uniform conducting skin of metallic aircraft keeps potential differences among structural elements low, thereby limiting the voltages which can be electrostatically coupled to interior electrical circuits. In practice, experimental measurements have shown magnetic and resistive components to be the most predominant.

In the previous program (ref. 1) an expression was derived for the induced voltage appearing at the open circuit terminals of any aircraft electrical circuit, as follows:

$$e_{oc}(t) = R_s i_L(t) + M\frac{di_L(t)}{dt} \qquad (1)$$

where

R_s = an effective structural resistance (ohms)

$i_L(t)$ = an expression for the time varying lightning current (amperes)

M = an effective inductive coupling factor (henrys).

Equation (1) permits expression of the open circuit-induced voltage in terms of the lightning current and two transfer

functions R_s and M. Equation (1) is the result of an effort to reduce the complete complex wing structure and circuitry to a simple, two terminal Thevenin equivalent circuit consisting of all linear components. The Thevenin equivalent circuit parameters representing each wing circuit were obtained from measurements of open circuit-induced voltages (e_{oc}) and short circuit currents (i_{sc}) at the terminals of the wing circuits. The reason for obtaining the Thevenin equivalent circuit is that the induced voltage seen by any load (appropriate avionics) connected to the circuit may then be calculated.

For equation (1) to be strictly correct for all time varying functions of i_L, the transfer functions R_s and M must be constant for all time, or at least for the time domains characteristic of natural lightning. In other words, values of R_s and M derived from a set of data taken at one lightning current waveshape should accurately describe the relationship between another lightning current waveshape and the corresponding voltage induced in the same circuit. In previous measurements, this was not often the case. For example, reference 1, tables X and XIV illustrate R_s and M reduced from the "fast" and "slow" lightning current waveshapes utilized in tests on both a position lamp and armament power supply circuit. (Note that R is given the subscript w to signify its application to a wing upon which these measurements were made.) These tables are reproduced here as tables I and II and illustrate a marked change in both R_w and M when the waveshape is changed from the slow (36 x 82 μsec) waveform to the fast (8.2 x 14 μsec) waveform. This data is from tests on an F89-J aircraft wing as described in reference 1.

This fact has been disconcerting since it diminishes the validity of the R and M transfer functions in predicting the voltage to be induced in a circuit by a lightning current waveshape other than the one being applied in a test. Yet, intuition and basic theory of linear systems indicates that the transfer functions should not be waveshape or time dependent. In this program, therefore, some effort was expended to further evaluate the initial derivation of R and M in an effort to discover the cause of the variations.

Skin Effect

In the previous analysis of reference 1, no account had been taken of the "skin effect" phenomena. As an introduction to skin effect, consider a long cylindrical conductor as shown in figure 1,

TABLE I - CALCULATED EFFECTIVE WING RESISTANCES AND MUTUAL INDUCTANCES FOR VARIOUS TEST CONDITIONS

Circuit L.050, Position Light
Conductor 2L10E18 and Airframe

i_L Wave Form:	Slow Wave Form (36 x 82 μs)		Fast Wave Form (8.2 x 14 μs)	
Stroke Location	R_w (microhms)	M (nanohenrys)	R_w (microhms)	M (nanohenrys)
1 Forward End of Tip Tank	450.0	16.3	700.0	4.25
4 Outboard Leading Edge	57.5	0.032	70.0	0.5
5 Trailing Edge of Aileron	25.0	2.75	-100.0	1.55
7 Center of Wing Surface	45.0	1.68	- 40.0	0.244
10 Inboard Leading Edge	40.0	0.022	60.0	0.31

(Formerly table X from ref. 1)

TABLE II - CALCULATED EFFECTIVE WING RESISTANCES AND MUTUAL INDUCTANCES FOR VARIOUS TEST CONDITIONS

Circuit S.220, Armament Power Supply
Conductor 2SF3886E20 and Airframe

i_L Wave Form:	Slow Wave Form (36 x 82 μs)		Fast Wave Form (8.2 x 14 μs)	
Stroke Location	R_w (microhms)	M (nanohenrys)	R_w (microhms)	M (nanohenrys)
1 Forward End of Tip Tank	0.625	-0.00028	2.5	0.0177
4 Outboard Leading Edge	0.50	-0.000224	2.5	0.0177
5 Trailing Edge of Aileron	0.75	-0.000336	0.88	0.0062
7 Center of Wing Surface	0.625	-0.00028	1.0	-0.00798
10 Inboard Leading Edge	0.50	-0.000224	0.25	0.00501

(Formerly table XIV from ref. 1)

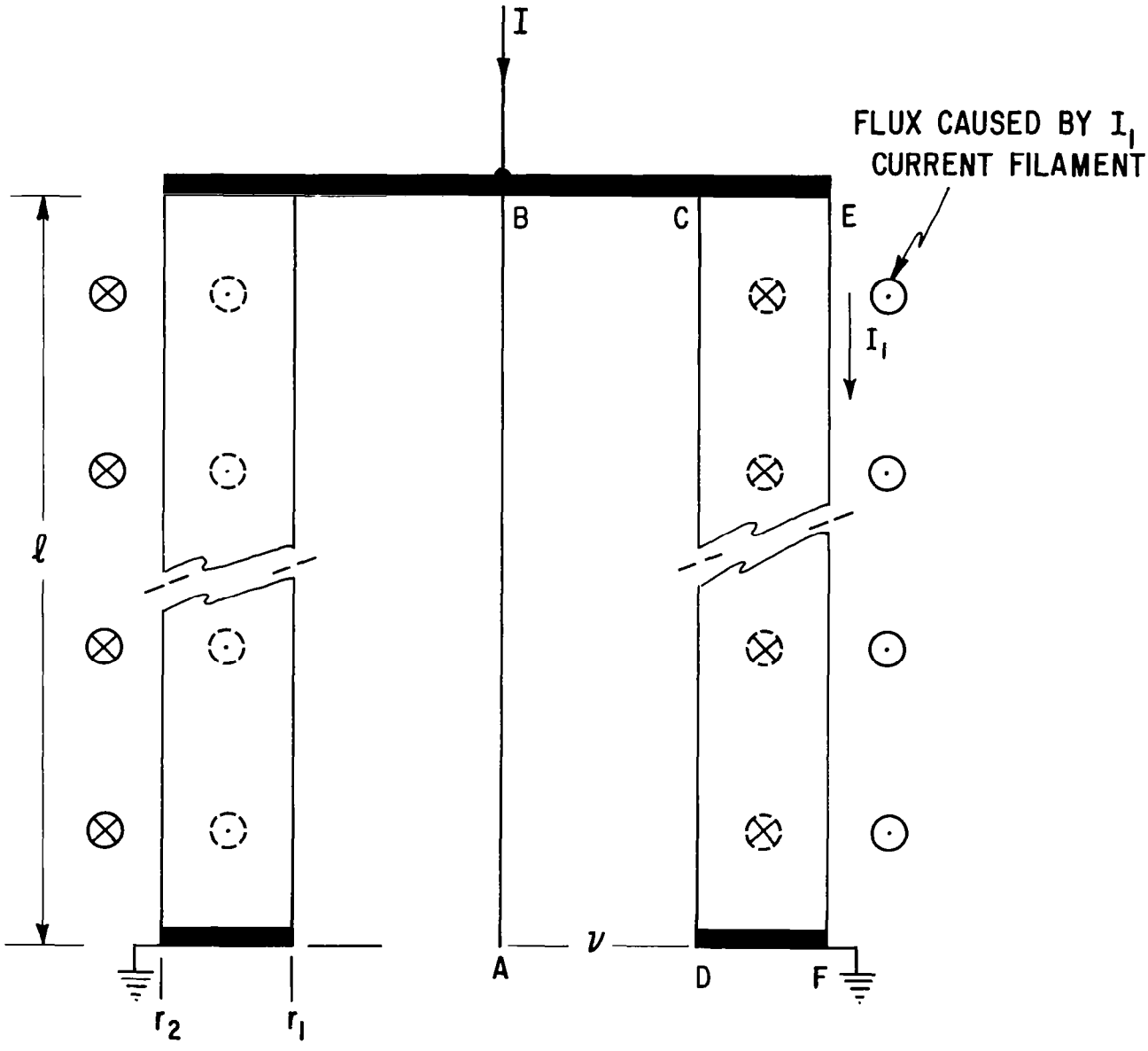

FIGURE 1 — IDEALIZED CYLINDER AND INNER CONDUCTOR

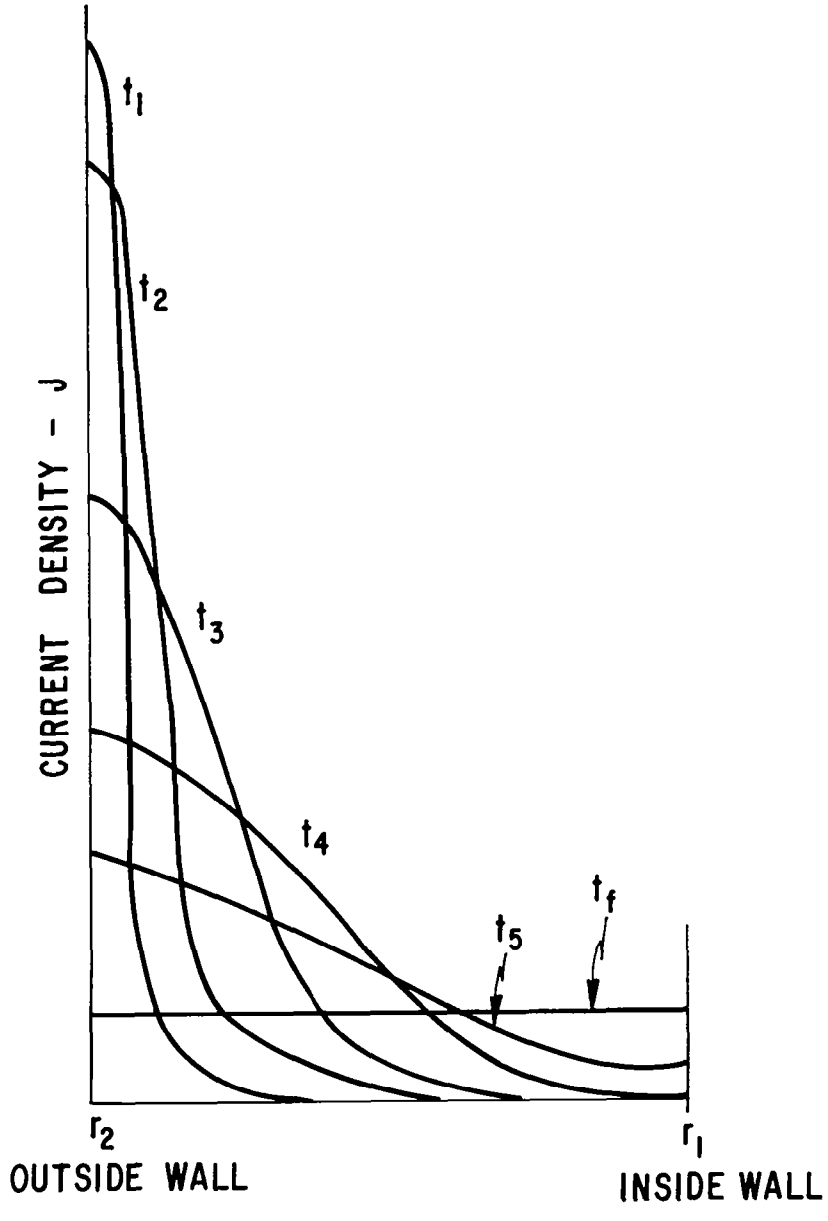

FIGURE 2 — CURRENT DENSITY IN CYLINDER WALL AT VARIOUS TIMES

whose length is long when compared to its diameter so that end effects can be neglected. If a step function of current, I, is injected into one end of this conductor, the total current will initially be confined to the outer surface.

This condition is the result of the magnetic fields, which initially force all the current to flow on the exterior surface of the cylinder, and is the phenomenon of skin effect. As time passes, however, the current will diffuse inward until eventually a condition of equilibrium is reached at t_f when the current density throughout the cylinder wall is uniform.

As the current diffuses into the cylinder wall, the current density at various times would probably appear as shown in figure 2. The current density is initially infinite and confined to an infinitesimally thin shell. For a final condition, t_f, the current density will be uniform throughout the wall thickness. At any time the area under the current density curve must equal the total input current. The current density at the inner wall will increase as shown in figure 3.

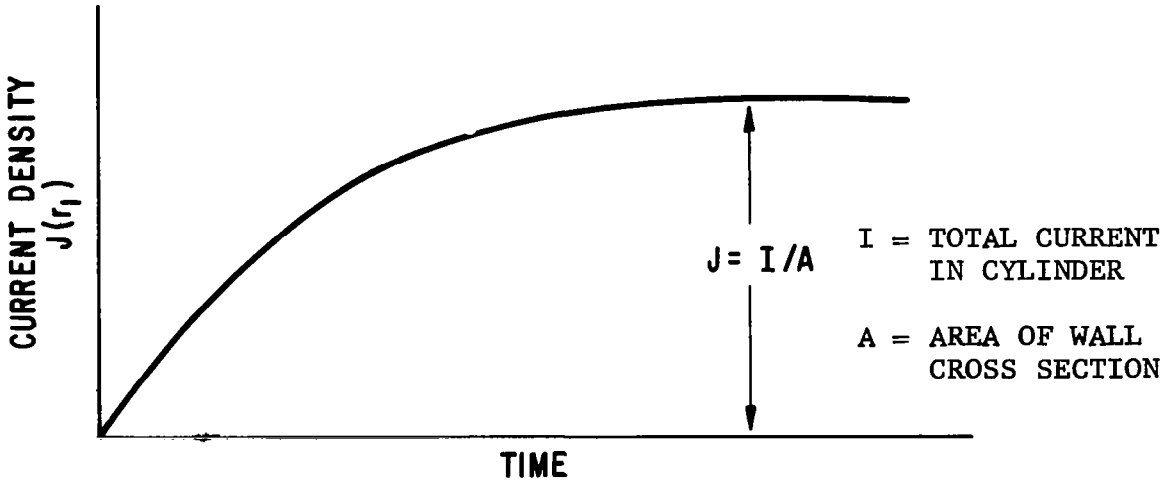

FIGURE 3 - CURRENT DENSITY AT INNER WALL OF CYLINDER OF FIGURE 1

Corresponding to this time variation of the current density must be a time varying magnetic flux. The magnetic flux will initially be external to the cylinder. As the current diffuses through the cylinder wall, so will a magnetic field diffuse through the cylinder.

If a conductor, AB, is placed along the center of the cylinder of figure 1, and is connected to the ungrounded end of the cylinder as at B, a voltage, v, will be developed between this conductor and the grounded end of the cylinder. This voltage is found by integrating the electric potential around the loop formed by the conductor and the cylinder wall (either the inner or the outer wall).

If the current density is assumed to be uniform over the length of the cylinder and one integrates around the loop, ABCD, formed by the conductor and the inner wall, the voltage v, developed between the conductor and the cylinder at the grounded end can be shown to be:

$$v = \int_0^{\ell} J_1 \rho \, d\ell = J_1 \rho \ell \tag{2}$$

where

J_1 = the current density on the inner wall at any time (t).

ρ = the resistivity of the conductor wall

ℓ = the total length of the cylinder.

If one evaluates the voltage developed in the loop formed by the conductor and the outer wall of the cylinder, the path encircles some magnetic flux and the equation becomes:

$$v = J_2 \rho \ell - \frac{d\phi}{dt} \tag{3}$$

where

J_2 = the current density at the outer wall at any time (t).

$\frac{d\phi}{dt}$ = the time derivative of the flux buildup in the cylinder wall.

Associated with the diffusing currents is the fact that the effective cross-section of current path is also changing. Because the

same total current is passing through a varying cross-sectional area, the effective resistance must also be varying, due to the relation:

$$R = \frac{\rho \ell}{a} \tag{4}$$

where

ρ = material resistivity (constant)

ℓ = length (constant)

a = area of current flow - time varying.

By similar reasoning, the magnetic flux appearing at the inside of the cylinder wall is also time variant. As a result, the resistive and magnetic components of any voltages induced between an internal conductor and the cylinder wall would be expected to be time variant due to skin effect in addition to being time variant due to the lightning current waveform and its differential as predicted by equation (1). Since equation (1) is applicable for circuits using the airframe as ground return, and is actually the line integral taken along the circuit conductor and the inside of the airframe as return, the coupling factors it sees are those apparent from the inside of the structure. These are related in turn to the current flowing on the inside of the structure wall and this current is itself a time varying function, beginning at zero and reaching a maximum sometime later.

According to Witt (ref. 2), the time constant of the build-up of voltage in a solid coaxial such as the cylinder of figure 1 will be approximately

$$T_M \approx \mu_0 \frac{\delta^2}{6\rho} \text{ (seconds)} \tag{5}$$

where

δ = wall thickness in meters

ρ = resistivity in ohm-meters

μ_0 = permeability of free space ($4\pi \times 10^{-7}$ henrys per meter)

The time constant thus varies with the square of the wall thickness of the cylinder, inversely with the resistivity of the material, and linearly with its permeability. Witt's derivation

was for a non-magnetic cylinder and, of course, the materials utilized in aircraft structures are nearly all non-magnetic. The derivation for an obround structure such as a wing has not been accomplished; however, that function is not expected to differ much from the cylindrical case of equation (5).

The point to be made by this discussion is that although the wing is not a cylinder it does have skin thickness and there is a time constant associated with the diffusion of the injected current throughout the wing.

The current i_L as used in equation (1) should, therefore, be the current appearing at the inner skin surface. In this case, equation (1) relating the induced voltage to the lightning current, i_L, should be modified to express the open circuit induced voltage, e_{oc}, in terms of the component of the lightning current appearing at the inside surface of the structure, as follows:

$$e_{oc} = R_s i_L(t) + M \frac{d(1-e^{-\alpha t})\ i_L(t)}{dt} \qquad (6)$$

where:

e_{oc} = induced voltage appearing across open circuit terminals

R_s = the effective structural resistance

M = an effective transfer inductance between the lightning current and the particular electrical circuit

$i_L(t)$ = lightning current (a time-varying function)

α = the reciprocal of the time constant of current penetration into the aircraft skin.

It will be noted that this is equation (1) with the factor

$$(1-e^{-\alpha t}) \qquad (7)$$

added to correct the total lightning current, i_L, for the portion of it appearing on the inside of the structure. The exponent, α, in the above expression is the reciprocal of the time constant of current penetration into the aircraft skin.

Since much of the resistance R_S is caused by bonds between various structural elements, these resistances must be lumped and the behavior of lightning currents flowing through them may not be identical to the diffusion process described for currents in a solid conducting skin. Therefore, the skin effect correction factor (eq. 7) has been omitted from the resistive term in equation (6) and the term R_S must therefore be defined as the "effective" resistance to lightning current flow, rather than the DC resistance.

The factor ($e^{-\alpha t}$) utilized to account for skin effect is not rigorously correct, but is instead an acceptable approximation of the skin effect diffusion process - a complex mathematical function not readily expressible in terms of the aircraft skin geometries of interest here. The exponential function used instead is more mathematically tractable and well within the bounds of accuracy imposed by other simplifications on these analytical procedures.

At time $t = 0$, expression (7) goes to zero and so does equation (6). At later times, (7) is increasing but always less than 1 until $t = \infty$. Thus, the effective "amount" of i_L in equation (6) is lessened at the earlier times and thus the factor (7) has the overall effect of changing the rate-of-rise of i_L in the expression for the magnetic component.

The magnitude of the time constant ($1/\alpha$) associated with current penetration of the F89-J wing would vary with location on the wing, and would be difficult to obtain rigorously because:

1. The wing skin thickness tapers from the center out to the leading and trailing edges.

2. The wing skin thickness tapers from the root end to the tip.

3. The current injection points vary.

4. There are discontinuities such as wheel well openings, antenna openings, and spacing between the wing tip and the wing tip fuel tank.

For the purpose of introducing skin effect into the ETCAL analysis to see if more consistent values of R and M would result, an average skin thickness was assumed for the entire wing, and calculations were run for thicknesses, δ, of .080" and .125" aluminum. Solving equation (5) for these thicknesses resulted in penetration time constants as follows:

For = .080" aluminum,

$$T_m = \frac{\mu_0 \delta^2}{6\rho} \tag{8}$$

$$= \frac{\left(4\pi \times 10^{-7} \frac{\text{henrys}}{\text{meter}}\right)\left(\frac{.01 \text{ meter}}{\text{cm}}\right)\left(\frac{.080 \text{ inches}}{.3937 \text{ inches/centimeter}}\right)^2}{6(2.828 \text{ microhm - centimeters})} \tag{9}$$

$$T_m = 30 \text{ microseconds.}$$

In a similar manner, T_m for a skin thickness of 0.125" is 74.2 microseconds. The F89-J wing skin thicknesses vary from 0.040" to 0.267" but the materials within which most of the wiring is located would appear to have 0.125" as a mean. Accordingly, the time constant,

$$T_m = 74.2 \text{ microseconds}$$

was used to derive α, where

$$\alpha = \frac{1}{74.2 \times 10^{-6}} \tag{10}$$

for use in equation (1).

If it is assumed that a period of 3 time constants must elapse before currents are equally distributed throughout the skin, this will be the time required for maximum current to appear on the inside surface of the skin. For lightning currents rising to crest and beginning their decay in less than this period the skin current penetration process will have the effect of slowing down the rise time of lightning current reaching the inside surface of the skin and diminishing its amplitude there. Thus, 0.125" skins with a time constant of 74.2 microseconds should provide greater shielding of internal electrical circuits against the effects of the 8 and 24 microsecond rising lightning currents simulated in the program, than an 0.080" skin whose time constant is only 30 microseconds.

ETCAL Computer Program

The ETCAL computer program described in reference 1 was revised to factor in skin effect, as expressed in equations (5) and (6). This program is presented in figure 4. A flow diagram illustrating the operation of this program is presented in figure 5. The derivation of the ETCAL analysis is otherwise the same as that presented in reference 1.

```
ETCAL
1    REM  THIS PRØGRAM CALCULATES THE RESISTIVE TRANSFER FUNCTIØN
2    REM  R AND INDUCTIVE TRANSFER FUNCTIØN M FRØM INDUCED
3    REM  VØLTAGES MEASURED IN A PARTICULAR CIRCUIT IN AN AIRCRAFT
4    REM  AS A FUNCTIØN ØF THE LIGHTNING CURRENT AMPLITUDE AND
5    REM  WAVEFØRM.  ØUTPUTS ARE:  R (ØHMS),  M (HENRYS), AND A
6    REM  TABLE ØF CALCULATED INDUCED VØLTAGES E(T) VS. TIME (T) FØR
7    REM  ALL TIME, BASED ØN R AND M.  E(T) IS IN VØLTS, T IN SECØNDS.
8    REM  INPUTS ARE:
9    REM  I1 = MAX AMPLITUDE (CREST) ØF LIGHTNING CURRENT  (IN AMPS)
10   REM  I4 = IMAX FØR EXPØNENTIAL LIGHTNING CURRENT FØRMULA (IN AMPS)
11   REM  A = ALPHA EXPØNENT FRØM THE LIGHTNING FØRMULA (IN 1/SECØNDS)
12   REM  B = BETA      "      "   "      "        "        "
13   REM  E1 = MEASURED ØPEN CIRCUIT INDUCED VØLTAGE AT LIGHTNING
14   REM       CURRENT CREST TIME (IN VØLTS)
15   REM  T2 = TIME ØF INDUCED VØLTAGE ZERØ INTERSECT (IN SECØNDS)
16   REM  P = DURATIØN ØF ØPEN CIRCUIT INDUCED VØLTAGE (IN SECØNDS)
17   REM  D = STEPS FØR THE INDUCED VØLTAGE PLØT (IN SECØNDS)
18   REM  M = DATA ØSCILLØGRAM NUMBER
19   REM  L = LIGHTNING STRØKE ATTACHMENT PØINT (ANY CØNVENIENT NØ.)
20   REM  C = AIRCRAFT CIRCUIT IDENTIFICATIØN NØ. (MUST BE NUMBERS ØNLY)
21   REM  S = TIME CØNSTANT ØF LIGHTNING CURRENT PENETRATIØN INTØ
22   REM       THE AIRCRAFT SKIN (IN SECØNDS)
100  READ I1,I4,A,B,E1,T2,P,D,M,L,C,S
107  PRINT "ACFT CIRCUIT NØ:"; C; "ØSC NØ:";M; "STRØKE LØC:";L
108  PRINT
110  LET R=E1/I1
115  PRINT
120  PRINT "R=";R
130  LET T=T2
150  GØ SUB 1200
160  LET M=-I*R/I3
165  PRINT
170  PRINT "M=";M
175  PRINT
180  PRINT" T (SEC)                E(T) VØLTS"
181  PRINT"***********                ************"
190  FØR T = 0 TØ P STEP D
200  GØ SUB 1200
210  LET E=I*R+M*I3
220  PRINT T,E
222  IF T>P-.5E-6 THEN 8990
230  NEXT T
1200 LET I=(I4/I1)*I1*(EXP(-A*T)-EXP(-B*T))
1300 LET I2=(I4/I1)*I1*(-A*EXP(-A*T)+B*EXP(-B*T))
1400 LET I3=(1/S)*I*EXP(-(1/S)*T)+(1-EXP(-(1/S)*T))*I2
1600 IF T<=P THEN 1900
1700 LET I=0
1800 LET I2=0
1850 LET I3=0
1900 RETURN
8990 PRINT
8991 PRINT
9000 GØ TØ 100
9100 DATA
9999 END
```

FIGURE 4 - COMPUTER PROGRAM "ETCAL" IN BASIC LANGUAGE FOR GE TIME SHARING COMPUTER SYSTEM

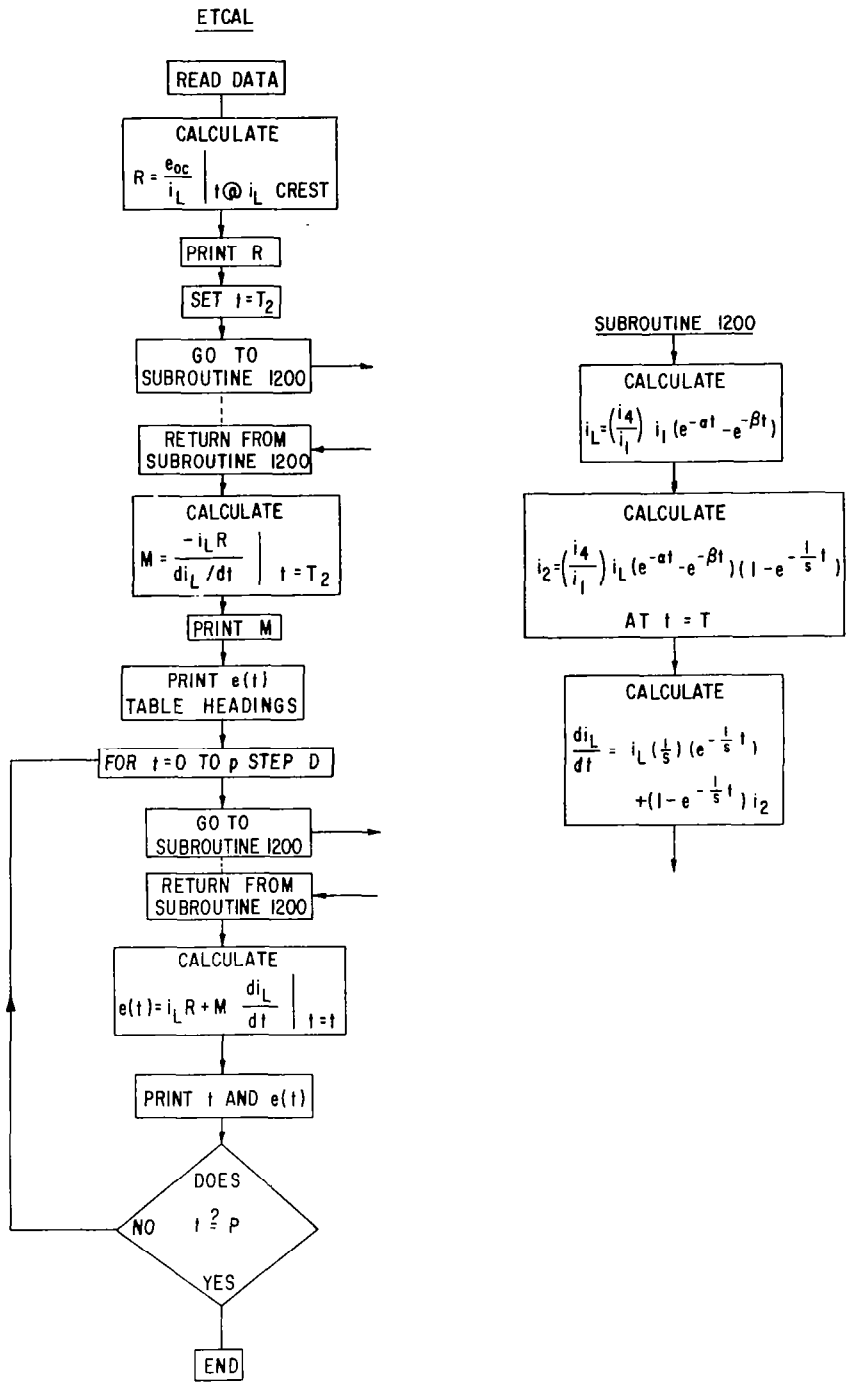

FIGURE 5 - FLOW DIAGRAM OF COMPUTER PROGRAM, ETCAL, TO CALCULATE R AND M TRANSFER FUNCTIONS FROM LIGHTNING INDUCED VOLTAGE MEASUREMENTS.

Transfer Function Analysis

In this program, measurements were made of voltages induced in various circuits in a complete F89-J fighter aircraft at the Naval Weapons Center, China Lake, California. These measurements, most of which are reported in General Electric Report No. SRD-72-065, "A Test Technique for Measuring Lightning-Induced Voltages on Aircraft Electrical Circuits" describing the experimental phase of this program, were made with low amplitude simulated lightning currents generated by the aircraft transient analyzer also developed under this program. The measurements at China Lake included circuits in which similar measurements had been made previously under the "full scale" tests described in reference 1 at the GE High Voltage Laboratory. Included were the position lamp (circuit No. L.050) and the armament power supply (circuit No. S.220). The values of R_w and M derived from the original ETCAL analysis of reference 1 are those presented in tables I and II of this report.

The revised ETCAL program of figure 4 was utilized for derivation of R_w and M from the China Lake data obtained in this program. At China Lake, an attempt was made to duplicate lightning current waveshapes utilized in the work of reference 1, however, the aircraft transient analyzer utilized to generate the simulated lightning current at China Lake utilized a linear resistive waveshaping element, whereas the full-scale lightning simulator used earlier utilized a non-linear resistor. While fairly similar waveshapes can be generated, sufficient differences do exist to affect rate-of-rise, induced voltage levels and the resulting ETCAL analysis. The lightning current waveshapes applied at China Lake included a 24 x 72 microsecond waveform (fig. 6) and a 8 x 20 microsecond waveform (fig. 7). These figures show the actual lightning current waveforms applied as well as a plot of the mathematical approximation used. The mathematical expression for each is also given in the figures, and these expressions were utilized in the ETCAL analysis.

The oscillograms of open-circuit induced voltages measured in the position lamp and armament power supply circuits are shown in figure 8. The remaining data required by the ETCAL program were taken from these oscillograms. Table IIIa represents the values of the transfer functions R_w and M calculated by the program from data generated by the 8 x 20 microsecond and 24 x 72 microsecond waveforms. The values of R_w and M calculated without consideration of skin effect for the same circuits and somewhat similar test conditions from reference 1 are also presented, in table IIIb, for comparison purposes.

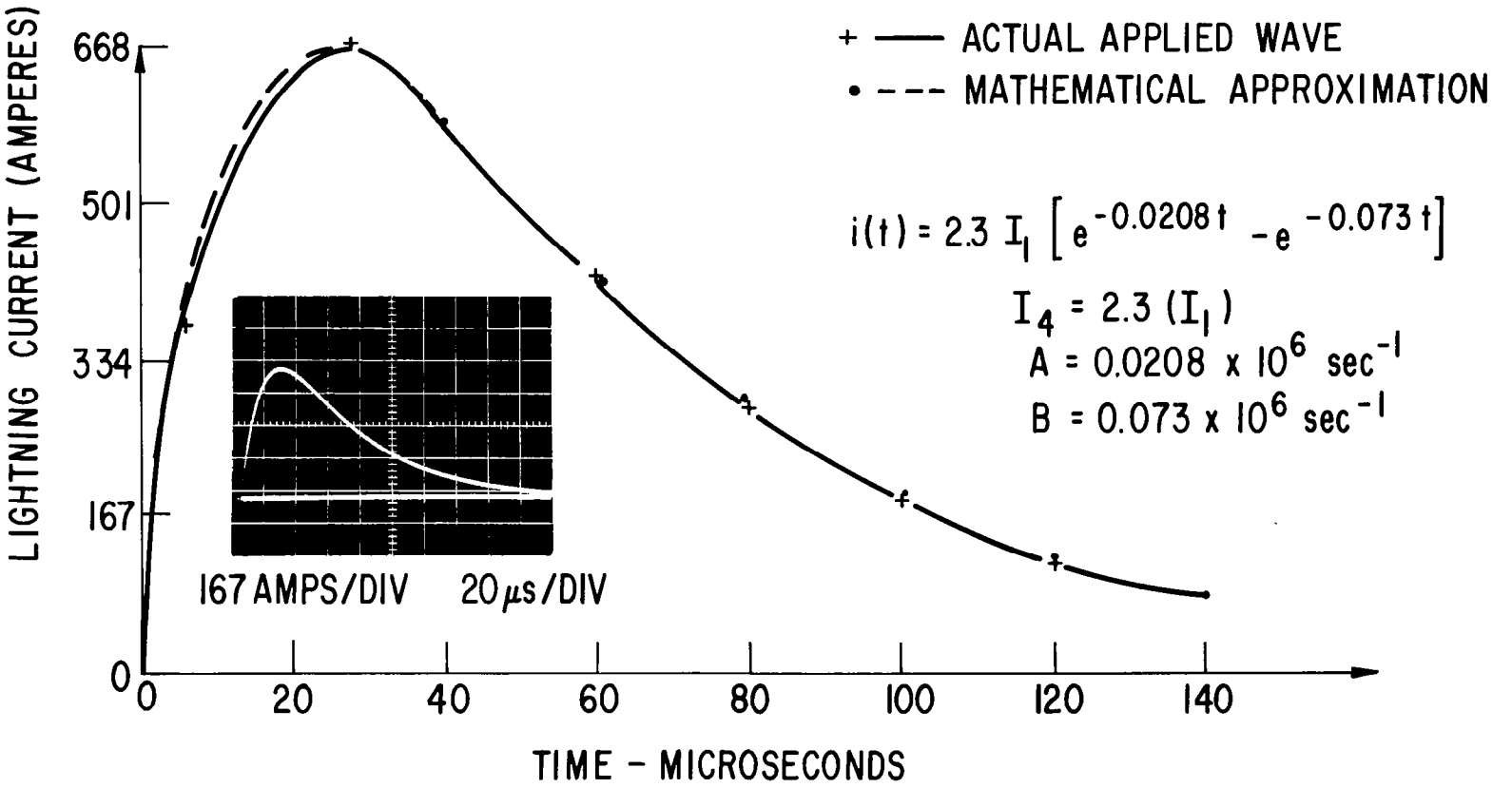

FIGURE 6 - 24 x 72 MICROSECOND SIMULATED LIGHTNING CURRENT WAVE SHAPE

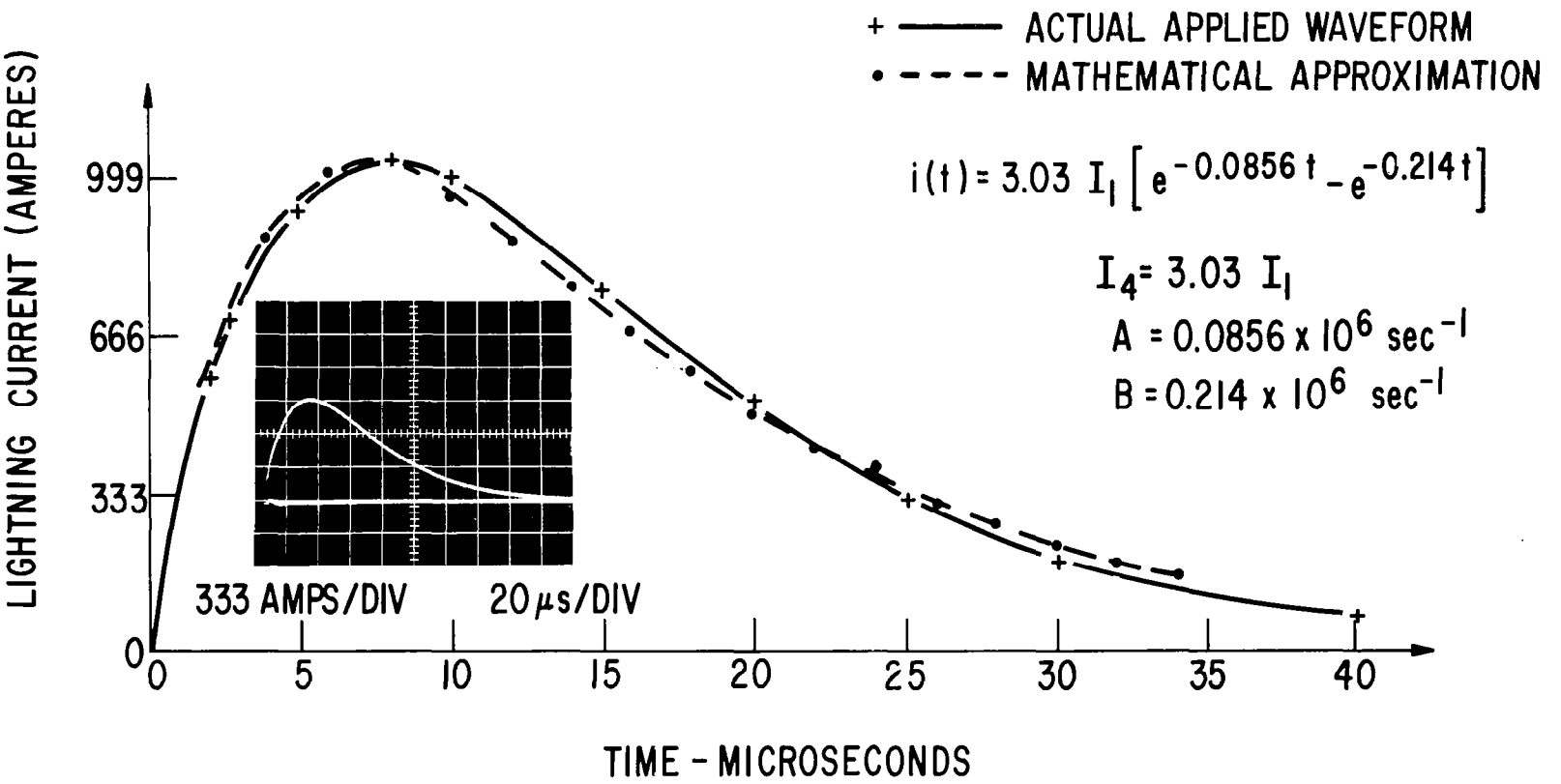

FIGURE 7 - 8 x 20 MICROSECOND SIMULATED LIGHTNING CURRENT WAVE SHAPE

SLOW i_L WAVEFORM
(24 x 72 μs, 666 AMPERES CREST
SEE FIGURE 5)

FAST i_L WAVEFORM
(6 x 20 μs, 1000 AMPERES CREST
SEE FIGURE 6)

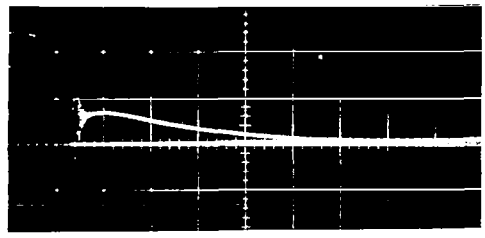

2 VOLTS/DIV e_{oc} 20 μs/DIV

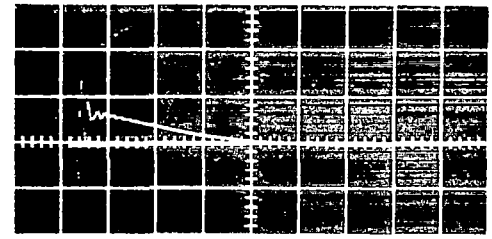

5 VOLTS/DIV e_{oc} 5 μs/DIV

CIRCUIT L.050, POSITION LAMP, WITH STROKE TO LOCATION I AT FORWARD END OF TIP TANK.

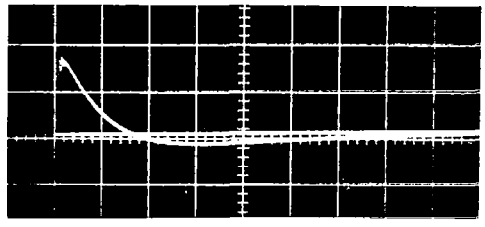

0.2 V/cm e_{oc} 20 μs/cm

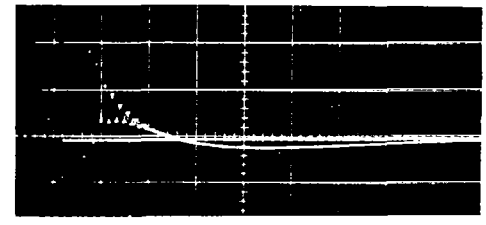

0.5 V/cm e_{oc} 5μs/cm

CIRCUIT L.050, POSITION LAMP, WITH STROKE TO LOCATION 4 AT OUTBOARD LEADING EDGE.

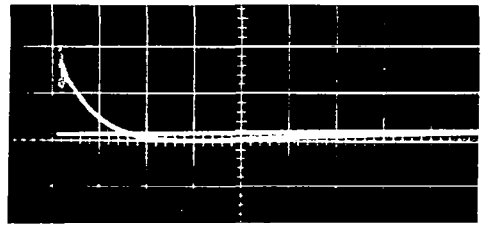

0.2 V/cm e_{oc} 20 μsec/cm

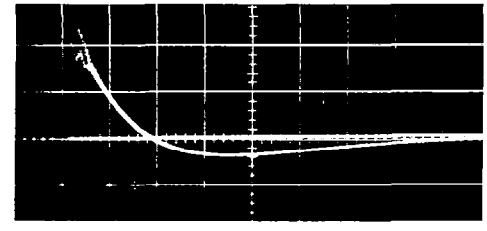

0.5 V/cm e_{oc} 5μsec/cm

CIRCUIT S220, ARMAMENT POWER SUPPLY, WITH STROKE TO LOCATION I AT FORWARD END OF TIP TANK.

FIGURE 8 - OPEN CIRCUIT VOLTAGES INDUCED IN THE POSITION LAMP & ARMAMENT POWER SUPPLY CIRCUITS OF AN F89-J AIRCRAFT AT NWC CHINA LAKE.

TABLE III - CALCULATED EFFECTIVE WING RESISTANCES AND MUTUAL INDUCTANCES, WITH AND WITHOUT CONSIDERATION OF SKIN AFFECT

a. Calculations by ETCAL of Figure 3 with Skin Affect
(From Measurements at China Lake on Complete F89-J Aircraft)

CIRCUIT	i_L Wave Form:	Fast Wave Form (8 x 20 μs)		Slow Wave Form (24 x 72 μs)	
	Stroke Location	R_w (microhms)	M (nanohenrys)	R_w (microhms)	M (nanohenrys)
L.050 Position Lamp (Conductor 2L10D18)	1 Forward End of Tip Tank	2600	157	1796	121
	4 Outboard Leading Edge	210	53.6	89.8	17.1
S.220 Armament Power Supply (Conductor 2SF3821G20)	1 Forward End of Tip Tank	50.0	5.10	59.9	8.98

b. Calculations by Original ETCAL of Reference 1 Without Skin Effect
(From Measurements at GE-HVL on Wing of an F89-J Aircraft)

CIRCUIT	i_L Wave Form:	Fast Wave Form (8.2 x 14 μs)		Slow Wave Form (36 x 82 μs)	
	Stroke Location	R_w (microhms)	M (nanohenrys)	R_w (microhms)	M (nanohenrys)
L.050 Position Lamp (Conductor 2L10D18)	1 Forward End of Tip Tank	700.0	4.25	450.0	16.3
	4 Outboard Leading Edge	70.0	0.5	57.5	0.032
S.220 Armament Power Supply (Conductor 2SF3886E20)	1 Forward End of Tip Tank	2.5	0.0177	0.625	-0.00028

Transfer Functions

After studying table III, it should be noted that for each circuit and stroke location there is much less of a percentage change in M resulting from the change in waveshapes than there was without the inclusion of skin effect in the analysis. Neither of the values of M calculated without skin effect is the same as the more consistent values calculated with skin effect. While the values calculated without skin effect accurately describe the induced voltage by equation (1) for the particular waveshape from which they were derived, they are inaccurate for other waveshapes. The degree of inaccuracy varies from case to case. If, however, M is reduced from data by the revised ETCAL program to include skin effect, it is apparent that together with R_w, it will more adequately describe the induced voltages generated by lightning current waveshapes other than the one whose data they were derived from, when used in equation (6).

Consistency in R_w and M in spite of lightning current waveshape variations is expected since these are fundamentally inactive circuit constants based on airframe material characteristics of resistivity, permeability, and geometrical distances which are not, at least within the range of current amplitudes considered here, functions of applied electrical stress. The fact that the program calculates a fundamentally larger value of M for the position lamp circuit than for the armament circuit is probably because the position lamp employs the airframe as a return and is connected via a low impedance (the bulb) to the airframe at its extremity, whereas the armament power supply conductor upon which this measurement was made is open-circuited at the pylon junction box. In the latter case, the magnetically induced voltage in the loop formed by the conductor and the airframe is probably countered somewhat by a capacitively coupled component which is effectively in series with the magnetic component, and of opposite polarity to it. This is a result frequently seen in high impedance or open-ended circuits (ref. 1).

When a second skin thickness of 80 mils was used to determine the skin effect time constant by (5), no significant changes resulted in R_w and M even though this diminishes the skin penetration time constant, T_m, to 30 microseconds from the 74.2 microseconds applicable to a thickness of 0.125 inch. This leads to the supposition that the time constant, while significant, is not a "sensitive" function when applied in equation (6). In view of the necessity to "average" many component skin thicknesses to arrive at a value for derivation of T_m in the first place, this

result is fortuitous if, in fact, it holds in most cases. Additional experience in application of the revised ETCAL program will have to transpire for this to be confirmed, however.

The lower resistance seen for the armament power supply circuit (S.220) when compared to the position lamp circuit (L.050) although for stroke location 1 at the forward end of the tip fuel tank in each case, can be accounted for when one considers that the armament circuit does not extend the full length of the wing. It should be remembered that the value R_w discussed here is the portion of the wing skin which serves as a return for the circuit.

It should be noted that R_w is not defined as the d-c resistance of the structure but is an "effective" resistance instead, probably arising from a very complex combination of bonding and material resistivities themselves. No attempt has been made, as yet, to derive this "effective" resistance in terms of the d-c equivalents of these resistivities, yet it is possible to see some basic relationships between values of calculated R_w and structural characteristics. The R_w calculated for the position lamp circuit for a lightning current entering the wing tip fuel tank is 10 to 20 times greater than that calculated for a stroke entering on the wing itself. This clearly indicates that the joint resistance between the tank and the wing adds a component to the induced voltage only when the lightning current flows through it. The joint resistance shows up in R_w derived by ETCAL accordingly, only when the lightning current must flow through this resistance. From table IIIa, the difference between R_w derived for a stroke to the tank (2600 μohms) and that derived for a stroke to the wing tip (210 μohms) must be the effective resistance of the joint itself. This would say that the joint has a resistance, by itself, of:

$$2600 - 210 = 2390 \ \mu\text{ohms}.$$

These values, from table IIIa, were derived from measurements made at China Lake on a complete F89-J aircraft, with the measurements made at the circuit terminals in the cockpit. The earlier data from measurements made on the F89-J wing alone, from table IIIb, result in an effective joint resistance of:

$$700 - 70 = 630 \ \mu\text{ohms}.$$

Different values accrue from the corresponding slow wave data on the same table, but the general relationships are the same.

Therefore, the "joint" on the F89-J at China Lake might be supposed to have a resistance three or four times that of the same part of the wing assembly tested earlier at the High Voltage Laboratory in Pittsfield. This difference may be explainable by the normal variation in mechanical joint bonding resistances, from one assembly to another, even though of the same design. However, the differences also might be attributable to the added bonding resistance of the wing-to-fuselage joint included in the lightning current flow path at China Lake but obviously not included at the High Voltage Laboratory. This bolted joint might have been responsible for the additional resistance of

$$\begin{pmatrix}\text{apparant joint } R_w \text{ at}\\ \text{China Lake}\end{pmatrix} - \begin{pmatrix}\text{apparant joint } R_w\\ \text{at HVL-Pittsfield}\end{pmatrix} = \tag{11}$$

$$(2390\ \mu\text{ohms}) - (630\ \mu\text{ohms}) = 1760\ \mu\text{ohms}.$$

Note that an even larger difference between corresponding values of M derived from the same two data sources exists, but this variation can be largely attributed to the inclusion of skin effect in the analysis of China Lake data. Study of equation (6) shows why this is so. With the factor $(1-e^{\alpha t})$ reducing the amplitude of i_L on the inside skin surfaces at any time t, a correspondingly larger value of M must appear to provide the same induced voltage amplitude as would be obtained from an uncorrected expression, as in equation (1). ETCAL calculates R_w by the same method for either case so the inclusion of skin effect in the China Lake analysis will not affect the R_w derivations.

If the wing-to-fuselage joint in the complete aircraft does indeed contribute to an increased R_w, then it follows that a lightning stroke flowing from the wing tip to fuselage, or to the opposite wing tip, would induce higher voltages in this and other circuits running from the wing to the fuselage where the measurements were made, as compared with measurements made on the same circuits at the wing root only. This was, in fact, the case in most instances where comparisons were made between China Lake data and earlier measurements on the F89-J wing alone.

SECTION II - A MATHEMATICAL MODELING TECHNIQUE FOR CALCULATING PROBABLE INDUCED VOLTAGES IN AIRCRAFT ELECTRICAL CIRCUITS

BASIC THEORY

Concurrently with the analysis of experimental data just described, work was begun during this program on development of a mathematical modeling technique to enable aircraft designers to calculate the probable magnitudes and waveshapes of lightning-induced voltages in proposed airframe and electrical circuit design and layout configurations. Such a tool would be very useful in enabling aircraft designers to anticipate the magnitude of the transfer functions associated with particular circuits and configurations associated with new aircraft designs, thereby permitting definition of the susceptibility of connected avionics and electric power system components to lightning-induced voltages. The need for protective measures can then be established.

For the purpose of this objective, a wing was chosen as the initial airframe to be modeled since a substantial amount of experimental data existed (ref. 1) against which to compare the accuracy of the model.

From equations (1) or (5), it is evident that if the transfer functions $\underline{R}$ and $\underline{M}$ for a particular circuit within an airframe are known, the voltage e_{oc} in the circuit can be calculated for any assumed lightning current waveform, $i_L(t)$.

Due to the fast rise and decay and short time duration of most lightning stroke currents, nearly all of this current will flow in the outer skins of metallic airframes rather than through internal spars and ribs, etc. Assuming that this is so, and also that the current flows uniformly in a lineal direction through a structure, its skin can be represented by a very large number, n, of infinitely small parallel current filaments. For an aircraft wing, this representation would be as shown in figure 9.

Assuming that the wing circuit pictured in figure 9 is "grounded" to the airframe at the outboard end of the wing, the voltage appearing between the inboard end of the conductor and the inboard airframe is equal to the line integral of voltage induced around a plane such as ABCD in figure 9.

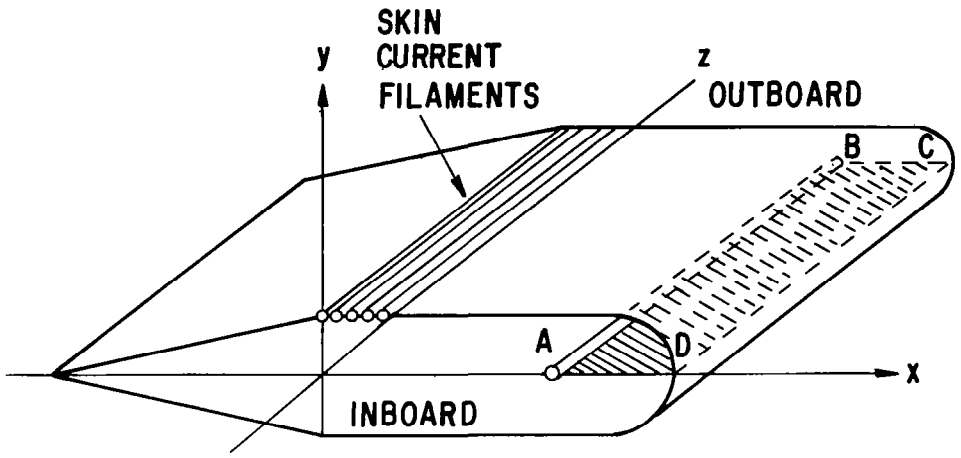

FIGURE 9 - ELECTRICAL REPRESENTATION OF WING

If lightning current flows on the wing skin and the skin has a finite resistance, then a resistive voltage drop will appear along CD and contribute to the total voltage along path ABCD. If i_L represents the entire lightning current, presumed to be equally distributed among all filaments, then the resistive voltage drop included along path CD is given by:

$$e_R = \frac{i_L}{n} R_n \tag{12}$$

In (12), R_n is the resistance of one current filament, equal to n times the total wing skin resistance, outboard to inboard.

The magnetically induced voltage is, by Faraday's Law, (ref. 3) equal to the time rate of decrease of the total magnetic flux linking the circuit. This is expressed as:

$$e_m = - \frac{d\varphi}{dt} \tag{13}$$

where

e = total EMF (volts)
φ = total flux (webers)
t = time (seconds)

If the voltage around the inboard circumference of the wing in figure 9 is assumed to be the same at all points, the voltage between the circuit conductor at A and the inboard circumference will also be the same at any point. Thus, the magnetic flux lines linking all planes defined by the particular wing circuit conductor (AB) and any longitudinal wing intersect will be equal. For purposes of calculation, it is convenient to choose a plane along the axis of symmetry (if available).

The portion of the magnetic flux passing through the plane ABCD generated by each of the skin current filaments must be determined and the total summarized in order to determine the magnetically induced voltage, e_m as defined in equation (13).

The magnetic flux density produced at some point, p, with respect to a current filament is defined by the Biot-Savart Law (5) as:

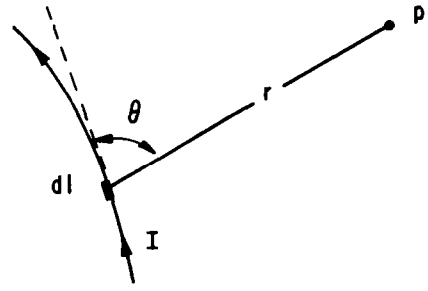

$$B = \frac{\mu I}{4\pi} \int \frac{\sin\theta}{r^2} \, dl \qquad (14)$$

where

I = current (amperes)
B = magnetic flux density (webers per meter^2)
l,r = dimensions in meters
μ = permeability of the medium (for air = $4\pi \times 10^{-7}$ henrys per meter)

The total flux, φn, passing through a given area is equal to the product of the area and the component of B normal to it. Thus,

$$\varphi_n = \iint B \cdot ds \tag{15}$$

where

φ_n = magnetic flux (webers) contributed by each skin current filament

In the wing circuit problem, the flux density, B, must be determined as a function of the current i_n and applicable geometry for each current filament along the wing skin, and integrated over the surface area defined by the plane ABCD, in accordance with equation (15).

Since the assumption has been made, for the present, that the total lightning current, i_L, is evenly distributed among the n skin current filaments, the voltage e_m can be written:

$$e_m = - \sum_{n=1}^{n=n} \frac{d\varphi_n}{dt} = - \frac{di_L}{dt} \sum_{n=1}^{n=n} M_n \tag{16}$$

where M is expressed in henries and i_L in amperes. Since e_m is related to di_L/dt by the function,

$$- \sum_{n=1}^{n=n} M_n = M \tag{17}$$

M operates as a transfer function expressing the magnetic-induced voltage in terms of the skin (lightning) current.

Computer Program

To calculate M for various wing geometries and circuit conductor positions, a computer program (WING) in BASIC language for use on the General Electric time-sharing computer system has been written. This program also calculates the resistive transfer function R_s based on skin dimensions and resistivity.

The computer program calculates the flux density, B, per ampere of lightning current, and the number of flux lines (webers) which link the plane ABCD from each individual skin current filament. The program performs the calculation of expression (18) for

the flux density, B, and the expression (19) for total flux lines, as follows:

$$B(r,\ell) = \frac{\mu I}{4\pi}\left[\frac{\ell}{r\sqrt{\ell^2 + r^2}} + \frac{L - \ell}{r\cdot\sqrt{(L-\ell)^2 + r^2}}\right] \tag{18}$$

$$\psi = \frac{\mu I}{2\pi}\left[\sqrt{D^2 + L^2} + L \log \frac{\sqrt{D^2 + L^2} - L}{D} - D\right]_{D=D_1}^{D=D_2} \tag{19}$$

where

ψ = magnetic flux (webers)

D, L, ℓ and r = dimensions in meters, as shown in figure 10.

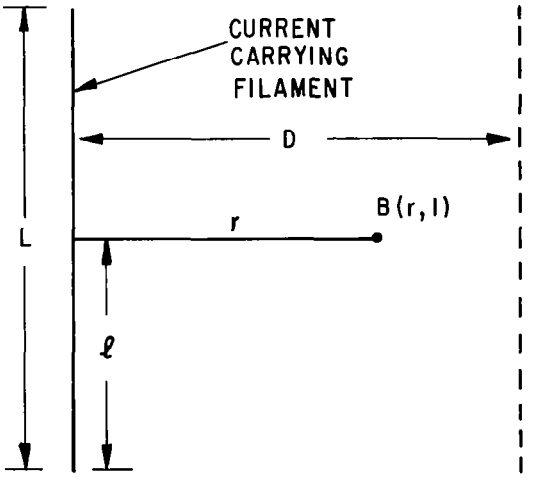

FIGURE 10 - DEFINITION OF DIMENSIONS OF EQUATIONS (18) and (19)

The program divides each equation by the lightning current to calculate the inductive transfer function, M, and the flux density, B, per ampere of lightning current.

The derivation of equations (18) and (19) from the Biot-Savart Law of equation (14) in terms of the definitions of figure 10 is presented in Appendix 1 of this report.

The computer program WING calculates the flux linking plane ABCD of figure 9 per ampere of skin current from each skin current filament by first calculating the distances of lines AB and CD from the filament, and identifying these as D_1 and D_2, respectively. Equation (19) is then solved for $D=D_1$ and for $D=D_2$ and the difference taken to achieve the flux passing between D_1 and D_2, which is, in fact, flux passing through the plane ABCD, as shown in the cross-sectional view of figure 11.

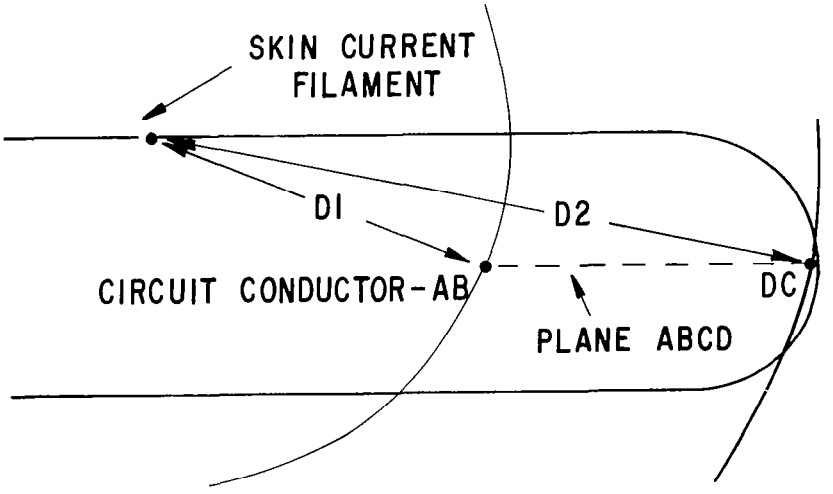

FIGURE 11 - CROSS SECTIONAL VIEW OF WING LEADING EDGE SHOWING DISTANCES UTILIZED IN CALCULATION OF MAGNETIC FLUX PASSING THROUGH PLANE ABCD BY EQUATION (19)

In figure 11 it is clear that the flux passing through ABCD generated by the skin current filament is equal to the flux, ψ_1, surrounding the filament out to a radius D_1 minus the flux, ψ_2, surrounding the filament out to D_2. Since all of this flux is generated by the same fraction of lightning current, (i_L/n), it follows that the fluxes ψ_1 and ψ_2 can be divided by (i_L/n) to obtain the corresponding inductive transfer function, M_n in henries, as follows:

$$M_n = \frac{\psi}{(i_L/n)} \qquad (20)$$

In WING ψ_1 is designated M8 and ψ_2 is designated M7. The program proceeds to calculate the flux passing through ABCD from each skin current filament. This contribution is given by

$$M_{ABCD} = (M7 - M8) \tag{21}$$

for each filament. It sums these quantities and the total is equal to the inductive transfer function between the wing and the conductor AB with airframe return. It designates this function M, with dimensions in henrys. M is, of course, purely a function of geometry and, therefore, not dependent on the amplitude of lightning current.

The flux density, B, is indeed a function of lightning current amplitude as well as geometry. It is calculated in accordance with equation (18) and, since it is not identical along the entire length, L, of the conductor AB, the program computes it for a point at the middle of L (half way down the wing). A slight program modification would permit it to be calculated for any other point along AB.

The program WING is presented in figure 12, and a flow diagram is presented in figure 13. Two subroutines are utilized in the program. "Subroutine 1200" calculates M and "subrouting 1000" calculates B. The wing geometry and other data required are listed at the head of the program. The geometrical quantities are defined by figure 14. Normally, the number of skin conductors required to reach a stable solution is sufficient when J is set equal to 1 centimeter, for a structure the size of an aircraft wing. More conductors may be required for accurate solutions near the leading and trailing edges, and in these cases values of J of 0.1 or 0.01 centimeters would probably provide authentic solutions. When the spacing between the circuit conductor AB and the inside of the wing becomes of the same order of magnitude as the spacing between skin filament conductors, the solutions calculated by the program are not considered authentic.

COMPARISON WITH MEASURED DATA

The program, WING, was used to calculate the transfer inductance, M, and the flux density, B, for aircraft circuit conductors assumed to be located at various positions on the horizontal axis of an F89-J wing. These calculations were made in the hopes that some idea of the authenticity of WING could be obtained by comparing the transfer functions calculated by WING with those

```
WING

1     REM  THIS PRØGRAM CALCULATES THE TRANSFER INDUCTANCE, M, AND
2     REM  THE TRANSFER RESISTANCE, R, RELATING INDUCED VØLTAGE IN
3     REM  A CIRCUIT ENCLØSED BY AN AIRCRAFT WING, TØ LIGHTNING
4     REM  CURRENT THRØUGH THE WING.  IT PRINTS ØUT THE (SELECTED)
5     REM  LØCATIØN ØF THE ENCLØSED CIRCUIT CØNDUCTØR, X1, AND THE
6     REM  TRANSFER FUNCTIØNS R AND M.  IT ALSØ PRINTS ØUT THE FLUX
7     REM  DENSITY, B, PER AMPERE ØF LIGHTNING CURRENT, AT A PØINT
8     REM  ØN THE ENCLØSED CIRCUIT ØNE HALF WAY DØWN THE WING LENGTH
9     REM  X1 IS IN CENTIMETERS
10    REM  R  IS IN ØHMS
11    REM  M  IS IN MICRØHENRYS
12    REM  B  IS IN WEBERS PER SQUARE METER PER AMPERE ØF LIGHTNING I.
13    REM  INPUTS ARE:
14    REM  S1 = AVERAGE WING SKIN THICKNESS (IN CENTIMETERS)
15    REM  R1 = THE SKIN MATERIAL RESISTIVITY (IN ØHM-CENTIMETERS)
16    REM  T  = THE HØRIZØNTAL WIDTH ØF THE TRAILING EDGE (IN CM.)
17    REM  C  = THE HØRIZØNTAL WIDTH ØF THE MAIN WING BØX (IN CM.)
18    REM  R  = LEADING EDGE RADIUS (ALSØ WING THICKNESS/2)  (IN CM.)
19    REM  J  = DISTANCE BETWEEN ASSUMED SKIN CØNDUCTØRS (USUALLY
20    REM       1, .1, ØR .01 CENTIMETERS)
21    REM  X1 = THE LØCATIØN ØF THE CØNDUCTØR BEING ANALYZED (IN
22    REM       CENTIMETERS FRØM THE AFT END ØF MAIN WING BØX)
23    REM  L  = THE LENGTH ØF THE WING (IN CENTIMETERS)
100   READ S1,R1,T,C,R
101   READ J,X1,L
105   LET B=P1*R+2*C+2*SQR(R↑2+T↑2)
106   LET N=B/J
107   LET P1 = 3.14159265
108   LET B = 0
109   LET B1 = 0
110   LET B2 = 0
111   LET B3 = 0

112   LET M = 0
113   LET M1 = 0
114   LET M3 = 0
115   LET M4=0
116   LET M5=0
117   LET M6=0
118   LET M7=0
119   LET M8=0
120   FØR Ø=(J/(2*R)) TØ ((P1/2)-(J/(2*R))) STEP (J/R)
130   IF X1<C THEN 212
140   LET D1=SQR((R↑2)+(X1-C)↑2-2*R*(X1-C)*CØS(Ø))
145   LET S=0.5*(D1+(X1-C)+R)
150   LET P=SQR((S-D1)*(S-(X1-C))*(S-R)/S)
155   LET U=P/(S-(X1-C))
160   LET X=2*ATN(U)
180   LET Z=Ø+X
190   LET D2=SQR(D1↑2+(R-(X1-C))↑2-2*D1*(R-(X1-C))*CØS(Z))
```

FIGURE 12 - COMPUTER PROGRAM "WING" IN BASIC LANGUAGE FOR GE TIME SHARING COMPUTER SYSTEM
(Continued next page)

```
195  GØ SUB 1000
196  LET B2=B1*SIN(Z+(P1/2))
200  GØ SUB 1200
210  NEXT Ø
211  GØ TØ 220
212  LET D2=SQR(R↑2+R↑2-2*R*R*CØS(Ø))
214  LET X=(P1/2)-(Ø/2)
216  LET D1=SQR((R+(C-X1))↑2+D2↑2-2*(R+(C-X1))*D2*CØS(X))
217  GØ TØ 195
220  FØR E=(J/2) TØ (C-(J/2)) STEP J
230  LET D1 = SQR(R↑2+(X1-E)↑2)
240  LET D2=SQR(R↑2+(R+C-E)↑2)
245  GØ SUB 1000
246  LET B2=-B1*((X1-E)/D1)
250  GØ SUB 1200
260  NEXT E
270  LET W=ATN(R/T)
280  FØR G=(J*CØS(W))/2 TØ T-((J*CØS(W))/2) STEP J*CØS(W)
290  LET Y=G*(R/T)
300  LET D1=SQR(Y↑2+(X1+T-G)↑2)
310  LET D2=SQR(Y↑2+(C+R+T-G)↑2)
315  GØ SUB 1000
316  LET B2=-B1*((X1+T-G)/D1)
320  GØ SUB 1200
330  NEXT G
340  LET A=S1*(P1*R+2*C+2*SQR(T↑2+R↑2))
350  LET R2=R1*(L/A)
360  PRINT "X1="X1;"M="M;"R2="R2
365  PRINT "B="B3
370  GØ TØ 1330
1000 LET B1=(.002/N)*((L/2)/(D1*SQR((L/2)↑2+D1↑2)))*2
1010 RETURN
1200 LET M1=(.002/N)*(SQR(D1↑2+L↑2)+L*(LØG(SQR(D1↑2+L↑2)-L)-LØG(D1)))
1220 LET M3=(-.002/N)*D1
1230 LET M4=(.002/N)*(SQR(D2↑2+L↑2))
1240 LET M5=(.002/N)*(-L)*(LØG(SQR(D2↑2+L↑2)+L)-LØG(D2))
1250 LET M6=(-.002/N)*D2
1260 LET M7=M1+M3
1270 LET M8=M4+M5+M6
1280 LET M=M+2*(M7-M8)
1282 LET B3=B3+2*B2
1290 RETURN
1300 DATA
1310 DATA
1330 END
```

FIGURE 12 - Continued

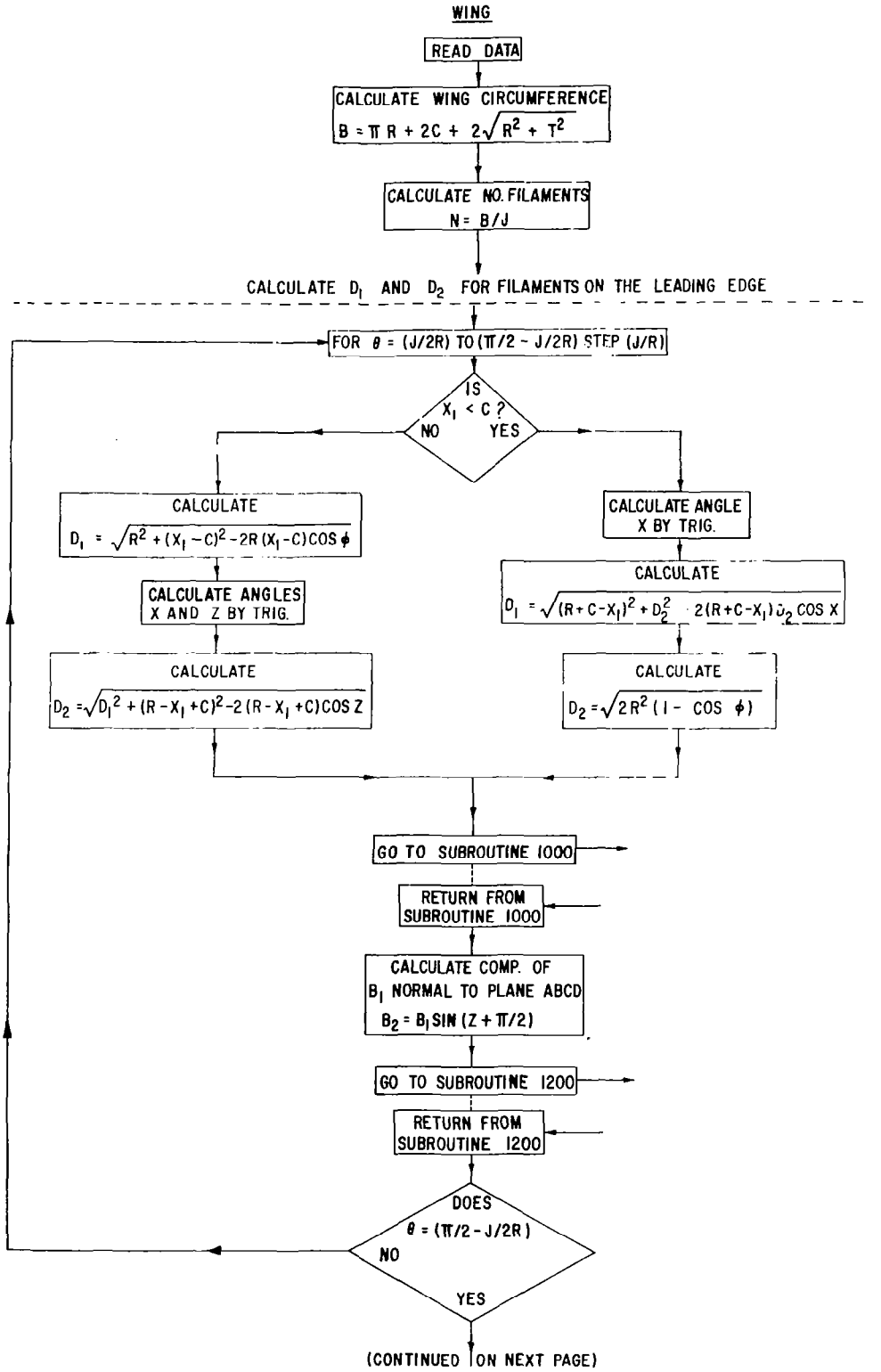

FIGURE 13 - FLOW DIAGRAM OF COMPUTER PROGRAM, WING, TO CALCULATE R AND M TRANSFER FUNCTIONS FOR AN AIRCRAFT WING

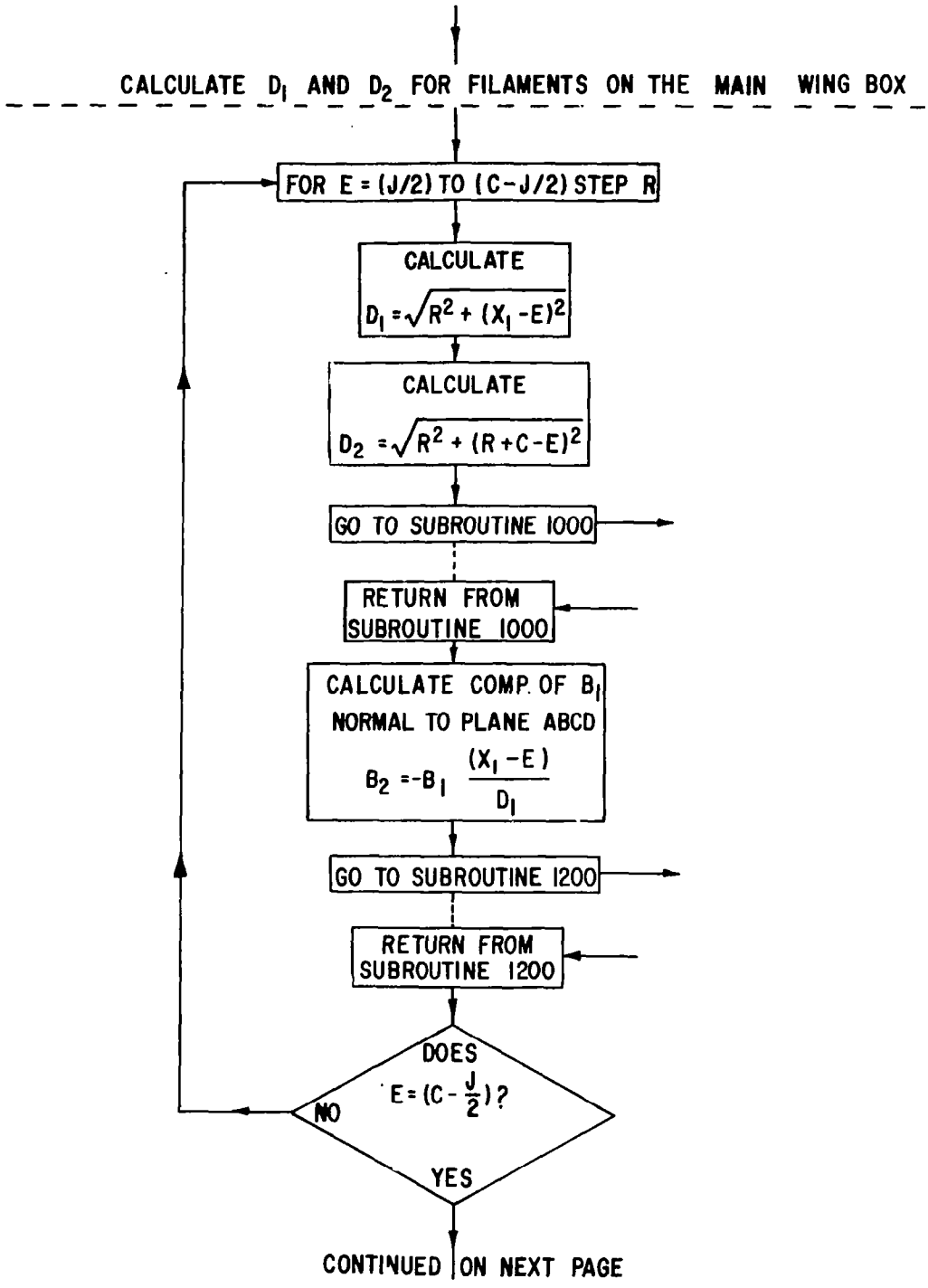

FIGURE 13-(CONTINUED)

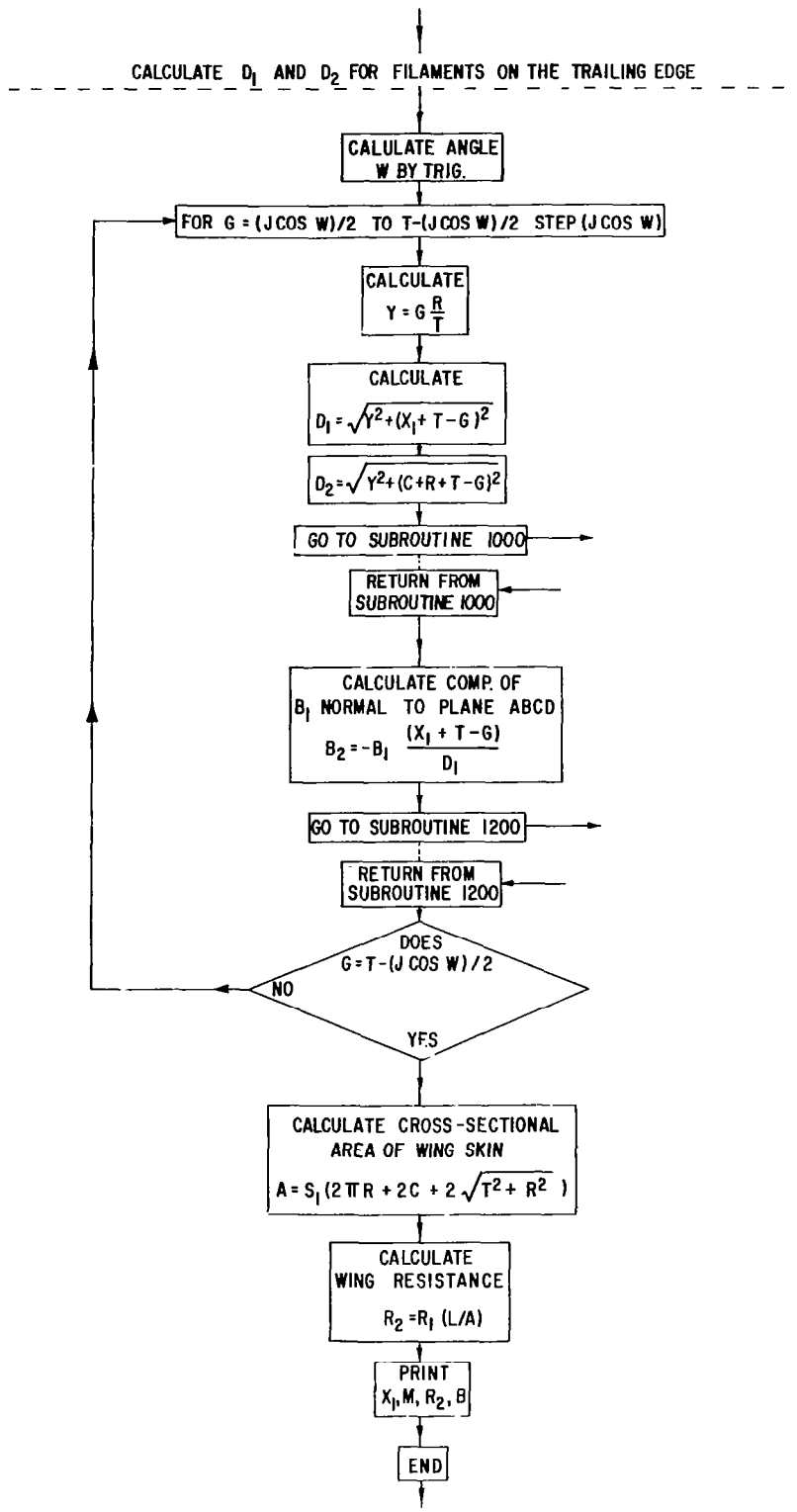

FIGURE 13 -(CONTINUED)

WING (CONT'D)

SUBROUTINES

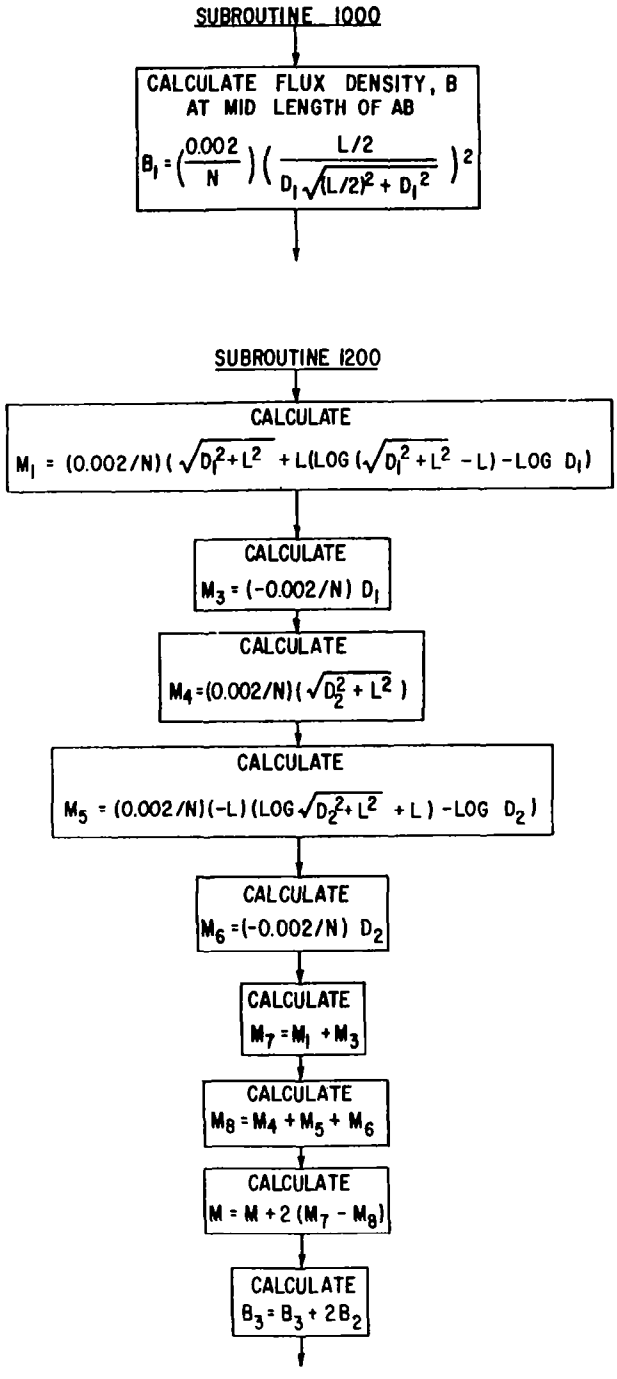

FIGURE 13 - (CONTINUED)

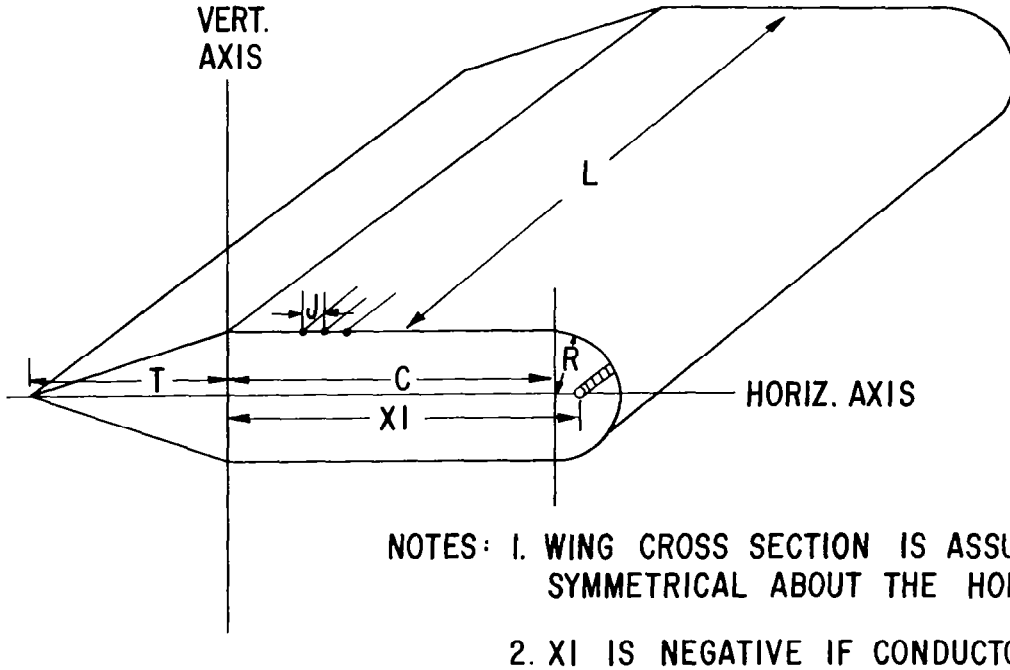

NOTES: 1. WING CROSS SECTION IS ASSUMED TO BE SYMMETRICAL ABOUT THE HORIZONTAL AXIS.

2. XI IS NEGATIVE IF CONDUCTOR IS PLACED AFT OF VERTICAL AXIS.

FIGURE 14 - GEOMETRICAL DATA ITEMS REQUIRED FOR WING COMPUTER PROGRAM

reduced from measured F89-J induced voltage data by ETCAL. Due to the basic geometrical definitions used in WING of figure 14, some simplification was necessary in the F89-J dimensions for input to the WING program. The F89-J wing is described in references 1 and 5. Basically, it is 680 centimeters long and tapers from about 46 centimeters down to about 15 centimeters thick at the center spar. Chord (less ailerons and flaps) distance tapers from 282 centimeters at the root to 193 centimeters at the tip. These dimensions were approximately averaged, after inspection of the wing, to determine the most realistic dimension inputs to WING.

The data inputs describing the modeled F89-J wing were:

S_1 (average skin thickness) = 0.318 cm

R_1 (skin material resistivity for aluminum) = 2.82×10^{-6} ohm-cm

T (horizontal width of trailing edge) = 107 cm

C (horizontal width of main wing box) = 240 cm

R (leading edge radius) = 20 cm.

Figure 15 is a plot of the values of transfer inductance, M, and flux density, B, calculated by WING for circuit conductors located at various positions from leading to trailing edges. There is some question as to whether a significant portion of the lightning current actually flows along the ailerons and flaps as it does through the skin covering the main wing box and leading edges. In cruise flight, with ailerons and flaps in a near 0^{o} position, the small gaps between ailerons and flaps may be arced over by the lightning current, providing a continuous path. In many other cases, however, this may not be so. Thus, the F89-J wing was modeled with and without the ailerons and flaps. When the program was run in the latter case, the dimension, T, was reduced to 1 centimeter (to avoid a discontinuity at T=0) and the aft spar was assumed to carry a proportionate amount of lightning current. Plots of M and B are presented in figure 15 for both cases. The transfer inductance, M, is plotted against the left scale which is in logarithmic increments. B, the flux density, is plotted against the right scale which is linear about a zero line shown dashed across the figure.

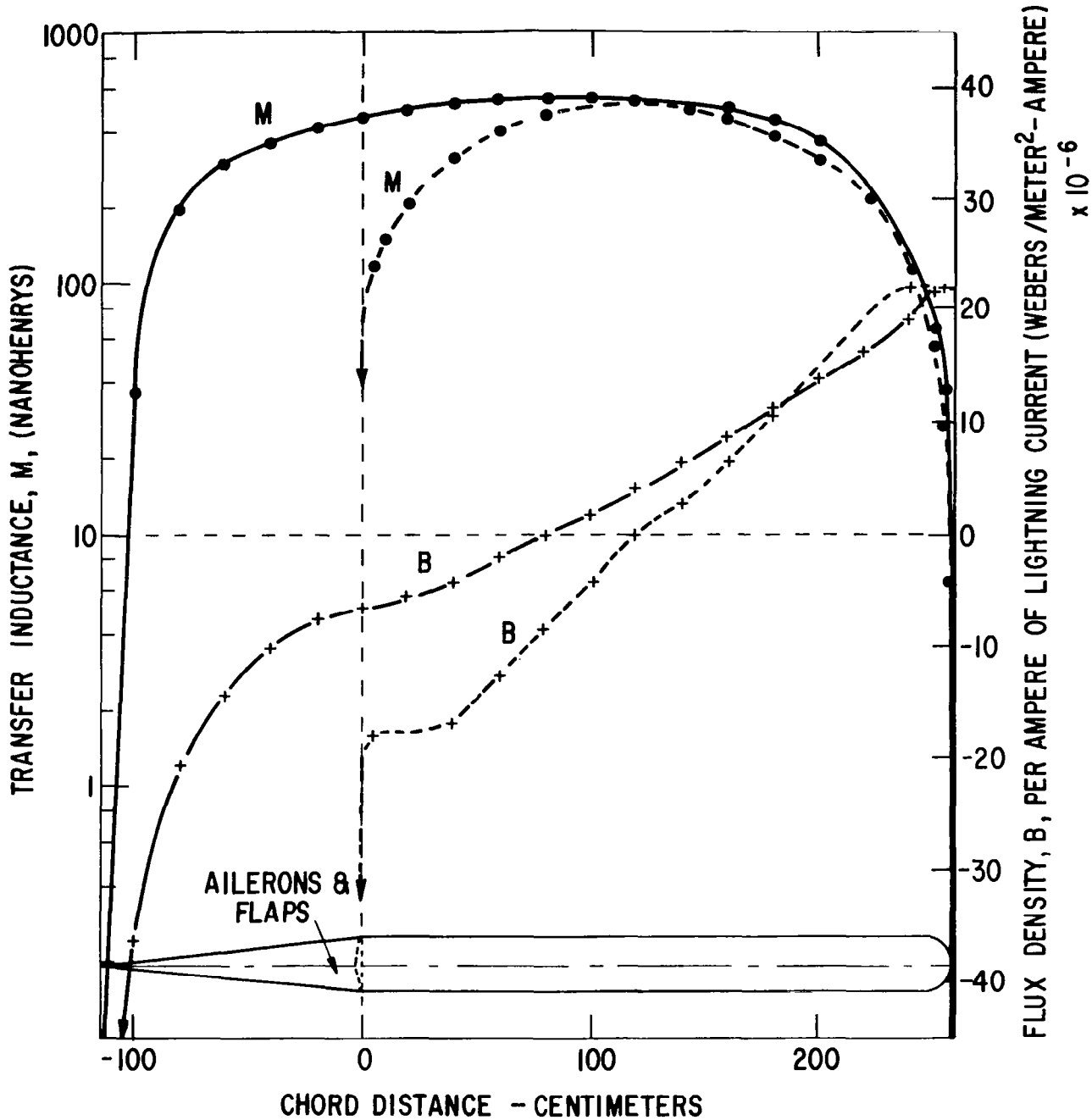

FIGURE 15 - CALCULATED VALUES OF TRANSFER INDUCTANCE, M, AND FLUX DENSITY, B, AT CONDUCTOR LOCATIONS ALONG THE AXIS OF SYMMETRY OF F89-J WING MODELLED BY WING COMPUTER PROGRAM.

Figure 15 shows that the value of the transfer inductance, M, varies from its lowest values (apparently approaching zero) near the leading and trailing edges, to a maximum near (but not at) the center of the wing box. The maximum transfer inductance calculated by WING is slightly more than 0.5 microhenry at locations around 100 centimeters from the aft main spar for this model, but the minimum is considerably less than this in regions more frequently utilized for running electrical circuits, such as the leading edge.

The resistance, R, is the same for all conductor locations since the entire airframe is involved as the return path for the circuit conductor, AB. This resistance only changes when the wing geometry changes, as when the ailerons and flaps are omitted from the model. The resistance values calculated were:

R (with ailerons and flaps included) = 7.9 microhms

R (without ailerons and flaps) = 10.35 microhms.

It is of interest to compare the values of M of figure 15 with those calculated from measured data by ETCAL, as presented on table III.

Table III indicates values of 53.6 and 17.1 nanohenrys (microhenrys x 10^3) for the position lamp circuit, which runs along the aft spar. For most of its travel it is on the inside (forward) of this spar, but opposite the flap it runs along the outside (aft) of the spar, slightly exposing it when the flap is down (flaps and ailerons were set about 20^o for the China Lake tests during which the measured data were taken). The location of the position lamp circuit forward of the spar is believed within a few centimeters of the spar. This circuit employs the airframe as return. These values of M fall within the range of transfer inductances calculated by WING for conductors within a few centimeters of the spar, when the flaps and ailerons were omitted from the model. This is logical since the amplitude of the driving voltage and currents generated by the aircraft transient analyzer is probably insufficient to cause sparking between flaps and ailerons, even if a full scale lightning flash could do so.

In the leading edge, circuit S220 (armament power supply) listed in table III may be compared with the data presented in figure 15, but it must be remembered that this circuit is not "grounded" to the airframe at the wing tip, as is the position

lamp circuit, and the circuit AB utilized for derivation of the model (eq. 13, etc). The capacitive coupling between an ungrounded circuit adds a component of capacitive voltage to the line integral around loop ABCD in figure 9, which may be of opposite polarity to the inductive voltage and thus appear to reduce the effective transfer inductance, M, calculated by ETCAL for table III, since ETCAL, in its present form, does not separate capacitive and inductive voltage components and transfer functions, but considers all non-resistive voltages to be the result of inductive coupling only. Thus, ETCAL calculates an M of between 5 and 9 nanohenrys, but a circuit located in about the same region within the leading edge of the modeled wing will have in the neighborhood of 50 nanohenrys, from figure 15.

Unfortunately, no circuits existed through the center of the F89-J wing upon which suitable measurements could be made for comparison with the WING calculations of figure 15. WING calculates the maximum transfer inductance to be in this region, as shown in table III, and it would be of interest to obtain measurements on an unshielded circuit in this location utilizing the airframe as return, for comparison with the calculations which show maximum transfer inductances of around 500 nanohenrys (0.5 microhenry). Such a value is greater than the transfer inductance calculated for any circuit in this or other induced voltage measurement programs, but since most electrical wiring is installed in the leading or trailing edges of wings, no measurements have been made in "center" circuits.

The values of magnetic flux density, B, per ampere of lightning current are also shown in figure 15. These calculations are made for a point half way down the wing, since flux density also varies along the axis of a conductor, in a wing of finite length. It is noteworthy that B is zero at locations where the transfer inductance, M, is greatest. B, of course, describes flux density at a point, whereas M describes total flux throughout an area. Thus, there is no inconsistency in this result. Instead, the result is telling us that for M to be greatest, the conductor should be located in a region where B is lowest, or zero. This applies for circuits utilizing the airframe as return only. It is expected that circuits with independent, parallel return paths, such as parallel pair or twisted pair circuits, will experience the greatest magnetic coupling and induced voltages where the flux density, B, is <u>greatest</u>. This is because only the area between conductors of the pair is now of importance in equation (13). WING would show this if it were modified to

calculate flux between wires of a pair instead of between a single conductor and the airframe.

Practically speaking, these results lead to two fundamental conclusions of importance to circuit and airframe designers:

1. To minimize magnetically induced voltages in circuits utilizing the airframe as return, these circuits should be placed in the leading and trailing edges, as close to the wing skin as possible.

2. To minimize magnetically-induced voltages in circuits with independent return, or in multi-conductor circuits where the voltage between any of them must be minimized, the conductors should be placed at a location near the center of the wing, where B is minimum.

Figure 15 shows that B does not vary significantly within about 40 centimeters from the well rounded leading edge. The program calculates a finite value of about 22 x 10^{-6} webers per square meter per ampere of lightning current in this region, and calculates a negative value of 5 times this level in the apex of the trailing edge (of ailerons and flaps). Here, the solution appears less stable and the validity of numbers less than 5 centimeters from the apex of the trailing edge is questionable.

The reader is reminded that all of the values of B and M plotted on figure 15, and the succeeding discussion are for conductor positions on the horizontal axis of symmetry only. These values should not be construed as valid for conductors very far above or below this axis. The flux density would be the same for equal distances above or below the axis, due to symmetry, but the degree of this variation is as yet unknown. WING can be extended to calculate M and B for <u>all</u> locations within the wing, and this should be done before WING is used in a thorough design analysis. It is not known if a similar result pertains, for example, when a conductor is placed near the top or bottom of the wing, as happens when the conductor is moved toward the leading or trailing edges. It is probable that B does, in fact, increase above and below the point on the axis of symmetry where it is zero, but the degree of this increase is not known.

The resistive transfer functions of 7.9 and 10.35 microhms with and without the ailerons and flaps respectively, are much

lower than the values presented in table III from ETCAL reductions of induced voltages in the F89-J, by a factor of five or more. This may be due to one or both of the following reasons:

1. The resistances calculated by WING are the d-c resistances, whereas those calculated by ETCAL for table III are effective resistances, which reflect skin effect. In the latter case, the effective resistance appears higher because the lightning current has not thoroughly diffused itself throughout the wing skin. While ETCAL has been modified to account for skin effect in the magnetic voltage component, it does not yet do so for the resistive component.

2. The resistance calculated by WING includes only the skin resistance itself, and not any resistances attributable to the tip tank joint or the wing root joint, or any other bonding resistances. The table III data most appropriately comparable to the WING calculations is for the position light circuit (L.050) with lightning current delivered to the outboard leading edge. The table IIIb data, for the wing only, is probably most comparable. R_w varies from 70 microhms for the 8.2 x 14 microsecond waveform to 57.5 microhms for the slower 36 x 82 microsecond waveform. Thus, it appears to decrease as the waveforms become longer and more time is available for diffusion of lightning current into the skin. If the time constant of diffusion throughout a 0.125 inch skin is in fact near 74.2 microseconds as given by equation (8), then only a small percentage of the total skin cross-sectional area is available for conduction by the time (at crest = 36 μs) that the effective R_w is calculated by ETCAL for the 36 x 82 microsecond waveform, as follows:

At $t = 36\ \mu s$,

$$\frac{A_{effective}}{A_{total}} = (1-e^{-\frac{t}{T}}) \qquad (22)$$

$$= (1-e^{-(36/74)})$$

$$= (1-\frac{1}{1.628})$$

$$= (1-.614) = 0.386$$

so the effective cross-sectional area is 38.6% of the total available area. Since resistance is inversely proportional to area,

this means that the d-c resistance calculated by WING should be

$$R_{dc} = 0.386\ (R_{effective})$$

If $R_{effective}$ is assumed to be the 57.5 microhms calculated by ETCAL for table IIIb, then the d-c resistance should be:

$$R_{dc} = (.386)(57.5 \text{ microhms})$$

$$= 22.2 \text{ microhms.}$$

This value is very close to the values of 10.35 and 7.9 microhms calculated by WING, when the simplifications utilized in the WING program are recalled.

CONCLUDING DISCUSSION

Two computer programs, ETCAL and WING have been developed to calculate the resistance and inductive transfer functions R and M from measured data or a drawing-board design model of an aircraft wing. The model program, WING, does not as yet account for design details such as openings, bonding or joint resistances, nonmetallic materials or the presence of ribs and spars, etc. Yet, lightning current apparently flows almost entirely in the aircraft skins, and the F89-J wing from which comparison test data was measured is completely metallic (aluminum) and of relatively simple design. Thus, the inductive transfer functions calculated by WING compare favorably with those calculated from actual induced voltage measurements by ETCAL.

Using the transfer functions, R and M, the voltage induced in any wing electrical circuit for which equation (6) is valid can be calculated for any assumed lightning current amplitude and waveshape. This can be done with transfer functions generated from previous measured data by ETCAL or from a drawing board design as modeled by WING. A short computer program, ECAL (not to be confused with ETCAL) has been prepared (fig. 16) to calculate e(t) for all values of t for any combination of lightning current parameters and transfer functions, skin thickness and resistivity. ECAL is programmed to accept R and M values calculated directly from WING or ETCAL. Thus, it must (and does) factor in skin effect in calculating the voltage induced in a circuit, by equation (6). The reader is cautioned, therefore, not to regard the geometrically calculated M in WING as being the <u>effective</u> transfer inductance in inducing the magnetic voltage component in the circuit. It is only correct when utilized in equation (6) or ECAL. This is because skin effect prevents all of the lightning current from being "seen" from inside of the wing, as discussed in Section I.

The similarity of the transfer functions derived from the analytical wing model with those derived by ETCAL from actual induced voltage measurements on the F89-J points out that the voltages induced in this aircraft's circuits have primarily been due to magnetic flux existing legitimately within the aircraft structure as a result of its geometry and not due to leakage

```
ECAL

1     REM THIS PRØGRAM, ECAL, CALCULATES THE VØLTAGE E(T) INDUCED BY
2     REM LIGHTNING IN AN AIRCRAFT ELECTRICAL CIRCUIT IF THE LIGHTNING
3     REM CURRENT AMPLITUDE AND WAVESHAPE, AND THE TRANSFER
4     REM INDUCTANCE, M, AND THE TRANSFER RESISTANCE, R, ARE KNØWN.
5     REM THE LIGHTNING CURRENT IS EXPRESSED IN BEWLEY'S DØUBLE
6     REM EXPØNENTIAL FØRMULA .   THE PRØGRAM PRINTS ØUT A TABLE
7     REM ØF TIMES AND CØRRESPØNDING INDUCED VØLTAGE ØRDINATES,
8     REM REPRESENTING THE TIME-VARYING INDUCED VØLTAGE, E(T).
9     REM REQUIRED INPUTS ARE:
10    REM   I4 = LIGHTNING AMPLITUDE CØEFFICIENT (KILØAMPERES)
11    REM   A  = FIRST LIGHTNING FØRMULA EXPØNENTIAL (1/MICRØSECØNDS)
12    REM   B  = SECØND   "       "          "          "
13    REM   C  = RECIPRØCAL ØF LIGHTNING CURRENT SKIN PENETRATIØN
14    REM        TIME CØNSTANT (1/MICRØSECØNDS)
15    REM   R  = TRANSFER RESISTANCE, FRØM (ETCAL) ØR (WING) (ØHMS)
16    REM   M  = TRANSFER INDUCTANCE, FRØM (ETCAL) ØR (WING) (HENRYS)
17    REM   P  = TIME DURATIØN ØF DESIRED E(T) TABLE (MICRØSECØNDS)
18    REM   T  = TIME INCREMENTS FØR DESIRED E(T) TABLE     "
19    REM SUGGEST THAT DATA ITEMS I4,A,B, AND C GØ IN LINE 190 AND
20    REM ITEMS R,M,P AND T GØ IN 200 FØR EASY VARIATIØN.
90    READ I4,A,B,C,R,M,P,D
100   FØR T=0 TØ P STEP D
110   LET I1=I4*(1E6)*((-A*EXP(-A*T))+B*EXP(-B*T)+(A+C)*EXP((-A-C)*T))
120   LET I2=I4*(1E6)*(B+C)*EXP((-B-C)*T)
130   LET I3=I1-I2
140   LET E1=R*I4*(EXP(-A*T)-EXP(-B*T))*(1-EXP((-C)*T))
150   LET E2=M*I3
160   LET E=E1-E2
170   PRINT T,E
180   NEXT T
190   DATA
200   DATA
210   END
```

FIGURE 16 - COMPUTER PROGRAM, ECAL, TO COMPUTE LIGHTNING-INDUCED VOLTAGE FROM LIGHTNING CURRENT PARAMETERS AND TRANSFER FUNCTIONS R_s AND M

flux coming through openings in the structure from outside. This fact is significant. It implies that plugging up, alone, of electrical discontinuities in the airframe may not be sufficient to reduce the succeptibility of electrical circuits within to acceptable levels. Treatment, instead, of individual circuits themselves may be required; either by modifications in circuit geometry, return method, or conductor shielding. The latter options, of course, become the only ones available when airframe skins are non-metallic.

ETCAL analyses were performed only on the circuits listed in table III. Similar analyses would probably be successful on most of the other circuits measured during the China Lake tests; however, attempts to utilize ETCAL to derive valid transfer functions from measurements on more complex circuits in this and other aircraft sometimes fail. ETCAL, it will be remembered (ref. 1), is fundamentally a method of deriving the Thevenin equivalent open circuit voltage source for a two-terminal pair, and Thevenin's theorem states that this can be accomplished regardless of the complexity of the circuit beyond the terminals, so long as it consists of a combination of active sources and passive, linear circuit elements. In the derivation of ETCAL, however, discrete data values are picked from time-varying oscillograms, and the validity of the resulting R and M values calculated depends greatly upon selection of the correct data points, as described in reference 1. The analysis, for example, requires that the point where the measured induced voltage, e_{oc}, crosses the zero line (t axis) be identified. To date, this point has been identified on the fundamental induced voltage trace with normally valid results. Some induced voltages, however, begin with a high frequency oscillation, usually decaying very early to the fundamental voltage waveform. These high frequency oscillations also cross the t axis, however, and might be considered as valid data points for ETCAL. Because <u>most</u> of these oscillatory events are thought to be secondary "ringing" in the electrical circuit and therefore not a part of the true induced voltage, the intersects from these oscillations have correctly been overlooked in the ETCAL analysis. It is possible, however, that some circuits receive, as a part of the induced voltage described by equation (1), a high frequency oscillatory component or some other component tending to obscure proper extraction of data for a correct ETCAL analysis. Some characteristics of circuits in which this seems to occur include:

1. circuits a large portion of which are in exposed areas, such as the cockpit area;

2. circuits with parallel branches in several different parts of the airframe;

3. circuits with complex filter networks included;

4. some circuits with non-linear elements, such as relay cores or motor armatures, etc.

There are other circuits which, when tested with certain lightning current waveforms, do not generate induced voltages which cross the t axis at well defined points. This may result when one component of the voltage is much greater than the other (usually the resistive component is greater than the inductive in these cases) or when a substantial capacitive component must be added in series with the resistive and magnetic components.

In all of these cases, it is believed that proper utilization of ETCAL or a subsequent improvement thereof will eventually enable derivation of valid transfer functions for all circuits. Further detailed study of these peculiar cases must be undertaken, however, before the ETCAL-type analytical procedure will become clear.

The success of this initial attempt to calculate possible induced voltages, via transfer functions, in wing electrical circuits suggests that further development can provide a computerized model capable of predicting all of the induced voltage information required by aircraft designers for avoidance of susceptibility or development of adequate protective measures in the design stage. Even in its present form, WING should be useful to designers in comparing the possible susceptibility of various wiring layout options in conventional wing designs.

Refinements which should be made in WING include handling of:

1. tapered dimensions

2. non-metallic skin sections

3. conductors within conduits or shields

4. separate return circuits

5. access doors and other openings

6. spars and ribs

7. more precise geometrical description of the modeled wing

8. conductors above and below the axis of symmetry

9. conductors whose length is less than that of the entire wing

10. provision for unequal lightning current distributions and current concentration at stroke attachment points on the airframe.

Some of these refinements are simple. Others will require more analytical work and computer time, but all will eventually be possible. In a similar manner, programs can be developed for other elements of an aircraft and added, electrically, to WING to enable a complete lightning-EMC analysis to be performed on an aircraft design. As each refinement is developed, its results should, where possible, be compared with results obtained from measured data to assure its validity. A relatively large volume of induced voltage data already exists for this purpose from recent measurements on several aircraft utilizing the aircraft transient analyzer.

The increasing use of advanced, solid-state microelectronics in aircraft avionics, coupled with the utilization of multiplexed transmission techniques and central avionics integration systems makes adequate protection from lightning-induced voltages a must if mission reliability and flight safety are to be maintained. Future use of solid-state electric power control techniques (SOSTEL) may also require that greater protection against lightning-induced voltages be designed into aircraft electric power distribution systems than is now the case. It is hoped that the analytical tools described herein are made use of for this purpose. The computer programs described are available from NASA Aerospace Safety Research and Data Institute or General Electric for this purpose. The programs will be kept up-to-date by the addition of refinements as these are developed.

APPENDIX I

1. Derivation of Equations (18) and (19) of Section II.

For the calculation of magnetic flux density, B, at a point, p, at some distance r from a current carrying wire of finite length, L, as shown in figure A1 below:

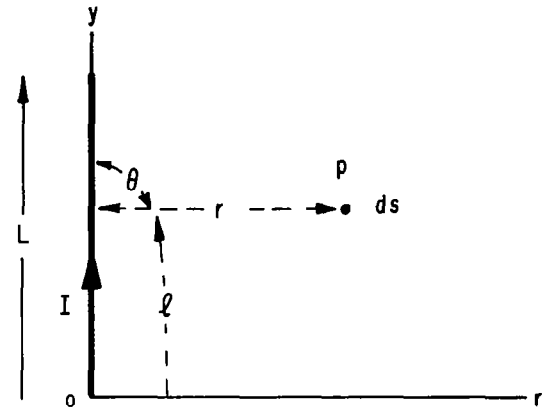

FIGURE A1

the Biot-Savart equation (ref. 4) gives:

$$B = \frac{\mu I}{4\pi} \int_0^L \frac{\sin\theta}{r^2} \, d\ell \qquad \text{(A1)}$$

where I = current (amperes)

B = flux density (webers per square meter)

L, r, ℓ = dimensions (meters)

μ = permeability (for air = $4\pi \times 10^{-7}$ henrys per meter)

Expressing the ($\sin\theta$) in terms of the geometry of figure A1, equation (A1) can be re-written:

$$B = \frac{\mu I}{4\pi}\int_0^{\ell} \frac{r}{\sqrt{(\ell-y)^2 + r^2}} \frac{1}{(\ell-y)^2 + r^2}\, dy \qquad 1^{st}\ \text{int.}$$

(A2)

$$+ \frac{\mu I}{4\pi}\int_0^{L} \frac{}{\sqrt{(y-\ell)^2 + r^2}} \frac{}{\left((y-\ell)^2 + r^2\right)}\, dy \qquad 2^{nd}\ \text{int.}$$

The first integral of (A2) can be re-written as equation (A3) and integrated by basic integral No. 173, page 71 of reference 6 as follows:

$$1^{st}\ \text{int.} = \frac{\mu I}{4\pi}\int_0^{\ell} \frac{r}{(\ell^2 + y^2 - 2\ell y + r^2)^{3/2}}\, dy \qquad (A3)$$

$$= -\frac{\mu I}{4\pi}\left[\frac{2r(2y-2\ell)}{\left(4\ell^2 - 4(r^2+\ell^2)\right)\sqrt{y^2 - 2\ell y + r^2 + L^2}}\right]_0^L \qquad (A4)$$

$$1^{st}\ \text{int.} = \frac{\mu I}{4\pi}\left[\frac{(y-\ell)}{r\ \ (y-\ell)^2 + r^2}\right]_0^L \qquad (A5)$$

where, for the basic integral No. 173 of reference 6,

$$a = 1, \quad b = -2\ell \quad \text{and} \quad c = (r^2+\ell^2).$$

The second integral of (A2) can be re-written and solved in the same manner as the first integral, as follows:

$$2^{nd}\ \text{int.} = \frac{\mu I}{4\pi}\int_0^{L} \frac{r}{(y^2 - 2\ell y + \ell^2 + r^2)^{3/2}}\, dy \qquad (A6)$$

$$= \frac{\mu I}{4\pi}\left[\frac{(y-\ell)}{r\sqrt{(y-\ell)^2 + r^2}}\right]_{\ell}^L \qquad (A7)$$

and it is seen that integral (A5) is evaluated along the y axis from the bottom of the wire at 0 in figure (A1) to ℓ, and integral (A7) is evaluated from ℓ to the top of the wire at L. This

integration gives B as a function of position in terms of ℓ at r as follows:

$$B(\ell,r) = \frac{\mu I}{4\pi}\left[\frac{\ell}{r\sqrt{\ell^2 + r^2}} + \frac{(L-\ell)}{r\sqrt{(L-\ell)^2 + r^2}}\right] \tag{A8}$$

Equation (A8) is thus an expression for the flux density, B, at some point at a distance from the current carrying wire. This is equation (18) in Section II of this report.

To find the total amount of flux, ψ, generated by this current, passing through an area bounded by lines parallel to the wire and distances D_1 and D_2 from it, it is necessary to integrate $B(\ell,r)$ over the area defined by these lines as shown below in figure A2.

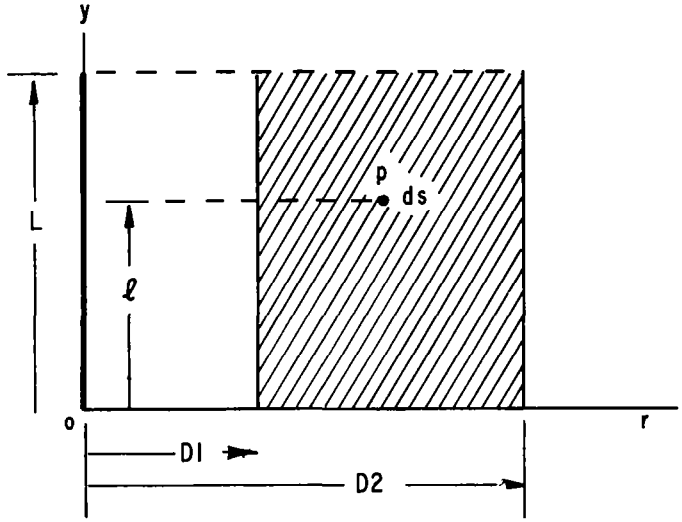

FIGURE A2

For this purpose the surface integral,

$$\psi = \iint B\cdot ds = \int_{D_1}^{D_2}\int_0^L B\cdot d\ell\ dr \tag{A9}$$

is to be solved. Substituting (A8) in (A9) we have

$$\psi = \frac{\mu I}{4\pi}\int_{D_1}^{D_2}\int_{0}^{L}\frac{\ell}{r\sqrt{\ell^2 + r^2}}\,d\ell\,dr \qquad \text{int. 1}$$

(A10)

$$+ \frac{\mu I}{4\pi}\int_{D_1}^{D_2}\int_{0}^{L}\frac{(L-\ell)}{r\sqrt{(L-\ell)^2 + r^2}}\,d\ell\,dr \qquad \text{int. 2}$$

Integrating first in the y direction from 0 to L, integral 1 of (A10) is solved by basic integral No.128 of page 67, reference 6, with

$$x = L, \qquad a = 1, \qquad c = r^2 \qquad \text{and } n = 1$$

as follows:

$$\text{int. 1} = \frac{\mu I}{4\pi}\int_{D_1}^{D_2}\left[\frac{\sqrt{\ell^2 + r^2}}{r}\right]_0^L dr \qquad (A11)$$

Integral 2 of (A10) can be re-written,

$$\text{int. 2} = \frac{\mu I}{4\pi}\int_{0}^{D_1}\int_{0}^{L}\frac{L}{r\sqrt{\ell^2 - 2L\ell + L^2 + r^2}}\,d\ell\,dr \qquad \text{int. 2a}$$

(A12)

$$- \frac{\mu I}{4\pi}\int_{0}^{D_1}\int_{0}^{L}\frac{\ell}{r\sqrt{\ell^2 - 2L\ell + L^2 + r^2}}\,d\ell\,dr \qquad \text{int. 2b}$$

and integral 2 is now divided into integral 2a plus integral 2b, as shown above. Integral 2a is solved by basic integral No.162, page 70 of reference 6 with

$$a = 1, \qquad b = -2L, \qquad c = (L^2 + r^2)$$

as follows:

$$\text{int. 2a} = \frac{\mu I}{4\pi}\int_{D_1}^{D_2}\left[\frac{L}{r}\log\left(2\ell - 2L + 2\sqrt{\ell^2 - 2L\ell + L^2 + r^2}\right)\right]_0^L dr \qquad (A13)$$

Evaluating integral (A13) between limits of $\ell = 0$ and L, equation (A13) becomes:

$$\text{int. } 2a = \frac{\mu I}{4\pi}\int_{D_1}^{D_2}\frac{L}{r}\log\left(2\sqrt{L^2 - 2L^2 + L^2 + r^2}\right) dr$$

$$- \frac{\mu I}{4\pi}\int_{D_1}^{D_2}\frac{L}{r}\log\left(-2L + 2\sqrt{L^2 + r^2}\right) dr \qquad \text{(A14)}$$

Simplifying,

$$\text{int. } 2a = \frac{\mu I}{4\pi}\int_{D_1}^{D_2}\frac{L}{r}\left[\log 2\sqrt{r^2} - \log\left(-2L + 2\sqrt{L^2 + r^2}\right)\right] dr \qquad \text{(A15)}$$

or

$$\text{int. } 2a = \frac{\mu I}{4\pi}\int_{D_1}^{D_2}\frac{L}{r}\left[\log 2r - \log\left(-2L + 2\sqrt{L^2 + r^2}\right)\right] dr \qquad \text{(A16)}$$

or

$$\text{int. } 2a = \frac{\mu I}{4\pi}\int_{D_1}^{D_2}\frac{L}{r}\log\left(\frac{r}{\sqrt{L^2 + r^2} - L}\right) dr \qquad \text{(A17)}$$

Integral 2b of (A12) is solved by basic integral No.164, page 70 of reference 6, with

$$a = 1, \qquad b = -2L, \qquad c = L^2 + r^2$$

$$\text{int. } 2b = -\frac{\mu I}{4\pi}\int_{D_1}^{D_2}\frac{1}{r}\left[\sqrt{\ell^2 - 2L\ell + L^2 + r^2} + \frac{2L}{2}\left(\log\left|2\ell - 2L + \sqrt{\ell^2 - 2L\ell + L^2 + r^2}\right|\right)\right]_0^L dr \qquad \text{(A18)}$$

Evaluating integral 2b between limits of 0 and L gives,

$$\text{int. } 2b = -\frac{\mu I}{4\pi}\int_{D_1}^{D_2}\left[\frac{1}{r}(r) + \frac{L}{r}\log 2r - \frac{1}{r}\sqrt{L^2 + r^2} - \frac{L}{r}\log\left(-2L + 2\sqrt{L^2 + r^2}\right)\right]dr \tag{A19}$$

Simplifying (A19) gives,

$$\text{int. } 2b = -\frac{\mu I}{4\pi}\int_{D_1}^{D_2}\left[(1) - \frac{1}{r}\sqrt{L^2 + r^2} + \frac{L}{r}\left(\log\frac{2r}{-2L + 2\sqrt{L^2 + r^2}}\right)\right]dr \tag{A20}$$

adding integral 2a and 2b by (A17) plus (A20) now gives integral 2 of (A10) as follows:

$$\text{int. } 2 = \frac{\mu I}{4\pi}\int_{D_1}^{D_2}\left[\frac{L}{r}\log\frac{r}{\sqrt{L^2 + r^2} - L}\right]dr \tag{A21}$$

$$-\frac{\mu I}{4\pi}\int_{D_1}^{D_2}\left[(1) - \frac{\sqrt{L^2 + r^2}}{r} + \frac{L}{r}\log\frac{r}{\sqrt{L^2 + r^2} - L}\right]dr$$

Now, the equation for ψ can again be written from (A10) as

$$\psi = \text{int. } 1 + \text{int. } 2 = (A11) + (A21) \tag{A22}$$

Evaluating (A11) between 0 and L, combining with (A21) and simplifying gives:

$$\psi = \frac{\mu I}{4\pi}\int_{D_1}^{D_2}\left(\frac{\sqrt{L^2 + r^2}}{r} - \frac{r}{r} + \frac{\sqrt{L^2 + r^2}}{r} - \frac{r}{r}\right) dr \qquad \text{(A23)}$$

or

$$\psi = \frac{\mu I}{4\pi}\int_{D_1}^{D_2}\frac{2}{r}\left(\sqrt{L^2 + r^2} - r\right) dr \qquad \text{(A24)}$$

Equation (A24) must now be integrated in the r direction from D_1 out to D_2 to achieve the entire magnetic flux passing through the area of interest as shown in figure A2. Equation (A24) can be re-written as:

$$\psi = \frac{\mu I}{2\pi}\int_{D_1}^{D_2}\frac{\sqrt{r^2 + L^2}}{r} dr - \frac{\mu I}{2\pi}\int_{D_1}^{D_2} dr \qquad \text{(A25)}$$

The first term of this equation is integrated by basic integral No.121, page 66 of reference 6 where

$$a = 1, \qquad \text{and } c = L^2, \qquad \text{from which,}$$

$$\psi = \frac{\mu I}{2\pi}\left[\sqrt{r^2 + L^2} + L\cdot\log\frac{\sqrt{r^2 + L^2} - L}{r} - r\right]_{D_1}^{D_2} \qquad \text{(A26)}$$

where r is evaluated from D_1 to D_2. The variable D is substituted in (A26) for r to become equation (19) of Section II.

REFERENCES

1. Lloyd, K.J., Plumer, J.A. and Walko, L.C., "Measurements and Analysis of Lightning-Induced Voltages in Aircraft Electrical Circuits", NASA CR-1744, February 1971.

2. Witt, H., "Response of Low Resistance Shunts for Impulse Circuits", Electroteknik, pp 45-47, 1960.

3. Kraus, J.D., "Electromagnetics", McGraw-Hill Book Co., Inc. p 287, 1953.

4. Ibid, p 148.

5. USAF Technical Order 1F-89J-2-1, "Handbook, Maintenance Instructions, General Airplane - F89-J Aircraft", Section I, 15 October 1956.

6. Burington, "Handbook of Mathematical Tables and Formulas", Handbook Publishers, Inc., Sandusky, Ohio, 1958.

NASA-Langley, 1974